수의학박사학위논문

Arsenic-induced Toxicity *In vitro* and *In vivo*

세포 및 생체에서의 비소 독성

2015년 8월

서울대학교 대학원

수의병인생물학 및 예방수의학(환경위생학)전공

김 수 희

Arsenic-induced Toxicity
In vitro and *In vivo*

세포 및 생체에서의 비소 독성

지도교수 류 덕 영

이 논문을 수의학박사학위논문으로 제출함
2015년 4월

서울대학교 대학원
수의병인생물학 및 예방수의학 (환경위생학)전공
김 수 희

김수희의 박사학위논문을 인준함
2015년 6월

위 원 장 박 재 학 (인)

부위원장 류 덕 영 (인)

위 원 김 용 백 (인)

위 원 조 성 범 (인)

위 원 구 현 옥 (인)

ABSTRACT

Arsenic-induced Toxicity *In vitro* and *In vivo*

Kim, Soohee

Laboratory of Veterinary Environmental Health

Veterinary Pathobiology and Preventive Medicine

Department of Veterinary Medicine

The Graduate School

Seoul National University

Arsenic is an environmental pollutant, and its toxicity has long been recognized. Arsenic has been associated with cancers of the skin, bladder, lung, kidney, and liver as well as with noncancerous conditions, diabetes and hepatopathy. Arsenic acts on cells through a variety of mechanisms, influencing numerous signal transduction pathways. It induces a variety of cellular effects such as apoptosis, growth inhibition, promotion or inhibition of differentiation and angiogenesis. Arsenic-induced responses vary depending on cell type, dose and its chemical form.

In the present study, the effect of arsenic on liver protein expression was analyzed by a proteomic approach in monkeys.

Monkeys were orally administered sodium arsenite (SA) for 28 days. The 2D-PAGE in combination with MS showed that the expression levels of 16 proteins were quantitatively changed in SA treated monkey livers compared to those of control-treated monkey. Specifically, the levels of two proteins, mortalin and tubulin beta chain, were significantly increased, and decreased were 14 proteins including plastin-3, cystathionine-beta-synthase, selenium-binding protein 1, annexin A6, alpha-enolase, phosphoenolpyruvate carboxykinase-M, erlin-2, and arginase-1. With regards to their functional roles, differential expression of these proteins may contribute to arsenic-induced liver toxicity, including cell death and carcinogenesis. Among the 16 identified proteins, four were selected for validation by Western blot and immunohistochemistry and many changes in the abundance of the toxicity-related proteins were also demonstrated in SA-treated human hepatoma HepG2 cells. In addition, to examine the involvement of c-Met and PI3K pathways in the SA-induced down-regulation of catalase, expression levels of catalase mRNA and protein were analyzed in HepG2 cells treated with SA and either an inhibitor of c-Met (PHA665752 (PHA)) or of PI3K (LY294002 (LY)). SA treatment markedly activated Akt and decreased the expression levels of both catalase mRNA and protein. Both PHA and LY attenuated SA-induced activation of Akt. PHA and LY treatment also prevented the inhibitory effect of SA on catalase

protein expression but did not affect the level of catalase mRNA. These findings suggest that SA-induced inhibition of catalase expression is regulated at the mRNA and post-transcriptional levels in HepG2 cells, and that the post-transcriptional regulation is mediated via c-Met- and PI3K-dependent mechanisms.

Arsenic is also known as an anticancer agent. Arsenic trioxide (ATO) was reported to induce remission in patients with acute promyelocytic leukemia (APL). Arsenic trioxide (ATO) has been used clinically to treat acute promyelocytic leukemia, but is less effective in solid tumors because the doses required to exert anti-cancer effects are extremely high. It is important to identify the mechanism associated with anti-cancer effects of ATO to reduce the side effects caused by high dose. This study was performed to elucidate the role of down-regulated Akt in the cell death induced by high dose ATO treatment. High-dose ATO caused a marked suppression of Akt expression in human cancer cell lines, including HepG2, HCT116, HeLa, and PC3 cells. In HepG2 cells, ATO induced apoptosis, which was prevented by pre-treatment with antioxidants, N-acetylcysteine (NAC) and ascorbic acid. Antioxidants attenuated the inhibitory effects of ATO on Akt expression at both the mRNA and protein levels. Down-regulation of Akt expression by ATO extended the suppression of Akt phosphorylation, and then activates GSK3β function by

decreasing its phosphorylation. GSK3β silencing using GSK3β-specific siRNA effectively prevented ATO-induced apoptosis, suggesting that activation of GSK3β via the suppression of Akt phosphorylation was critical in the ATO-induced apoptosis. The results indicate that GSK3β may be expected to become a new approach to use ATO for the treatment of solid tumors, such as hepatocellular carcinoma.

The present study about the arsenic-induced regulation of proteins with their critical roles may provide the specific mechanisms underlying SA-induced toxicity. Moreover, comprehensive study on the biology of ATO could help in developing ATO-based therapeutic interventions against solid tumors including hepatocellular carcinoma.

Keywords: Arsenic, Toxicity, HepG2 cells, Monkey liver, ATO, Chemotherapy
Student Number: 2008-21731

LIST OF CONTENTS

LIST OF FIGURES

LIST OF TABLES

LIST OF ABBREVIATIONS

AA	ascorbic acid
APL	acute promyelocytic leukemia
ATO	arsenic trioxide
CBS	cystathionine beta-synthase
DMSO	dimethylsulfoxide
ELISA	enzyme-linked immunosorbent ssay
FBPase	fructose-1,6-bisphosphatase
G6Pase	glucose-6-phosphatase
G6PD	glucose-6-phosphate dehydrogenase
GPx	glutathione peroxidase
GR	glutathione reductase
GSH	glutathione
HCC	hepatocellular carcinoma
HO-1	heme oxygenase-1
HRP	horse-radish peroxidase
IHC	immunohistochemistry
LY	LY294002
MT1	metallothionein 1
MTT	3-(4,5-Dimethylthiazol-2-yl)-2,5-diphenyl-tetrazolium bromide
NAC	N-acetylcystein
NO	nitricoxide
p-Chk2	phospho-Chk2
PCB	pyruvate carboxylase

PCNA	proliferative cell nuclear antigen
PEPCK	phosphoenolpyruvate carboxykinase
PHA	PHA665752
PI3K	phosphatidylinositol 3-kinase
PTEN	phosphatase and tensin homolog
ROS	reactive oxygen species
RT-PCR	Real time reverse transcriptase polymerase chain reaction
S.D.	standard deviation
SA	sodium arsenite
SBP	selenium-binding protein
SDS	sodium dodecyl sulfate

LITERATURE REVIEW

1. Introduction

Arsenic is the 33rd element of the periodic table of the chemical elements and is formally classified as a metalloid, i.e., it has characteristics of both metals and nonmetal. Arsenic was isolated in A.D. 1250 by Albertus Magnus, and has been used in medicine, agriculture, livestock, electronics, industry and metallurgy [1−3]. It has been a center of controversy in human history. In fact, the word "arsenic" is synonymous with poison, as a consequence of its long and nefarious history [1].

Arsenic from anthropogenic sources is widely distributed in water, soil and air, and its abundance ranks 20th in the Earth's crust, 14th in the seawater, and 12th in the human body [4]. It is a component of more than 245 minerals and exists in three allotropic forms, α (yellow), β (black), γ (grey). The γ form is a semimetal and also the most stable form [4]. Arsenic occurs mainly in the +5 (arsenate) or +3 (arsenite) oxidation states, and capable of forming both inorganic and organic compounds in the environment or human body [5]. It combines with oxygen, chlorine, and sulfur to form inorganic arsenic compounds in the environment, and with carbon and hydrogen to form organic arsenic compounds in animals and plants.

Arsenic has generally been considered as a potent human carcinogen based on epidemiological studies, which indicated a

positive relationship between the presence of inorganic arsenic in drinking water and an increased risk of skin cancer. Arsenic-contaminated groundwater, in which measured arsenic concentrations reached up to 1,000 μg/L, had severe effects on the health of the populations in Bangladesh and West Bengal [6-8]. To prevent this in the future, the WHO recommended limit for arsenic in water is 10 μg/L. However, arsenic is also known as an anticancer agent [9]. Arsenic trioxide (ATO) was reported to induce remission in patients with acute promyelocytic leukemia (APL) in China in the 1970s [10].

Arsenic acts on cells through a variety of mechanisms, influencing numerous signal transduction pathways and resulting in diverse cellular effects that include apoptosis, growth inhibition, promotion or inhibition of differentiation, and angiogenesis. Arsenic-induced responses vary depending on the cell type, arsenic species, and length and dose of exposure [11]. Although various mechanisms have been proposed to explain the effects of arsenic, no unified agreement has been reached.

2. Arsenic metabolism

A broad range of susceptibility to arsenic exists among individuals and this variation may be related to differences in metabolism [12]. Arsenic usually enters the body in the

trivalent inorganic form (asrenite) via a simple diffusion mechanism [13]. After absorption, arsenic compounds are metabolized via methylation by enzymatic transfer of the methyl group from S-adenosylmethionine to arsenite to form monomethylarsonic acid (MMAV), which is then reduced to monomethylarsonous acid. Arsenate, arsenite, and their methylated metabolites, MMAV and dimethylarsinic acid (DMA) have all been found in hamster liver following arsenate exposure [14]. Methylation occurs primarily in the liver and to a lesser extent in other organs such as the kidney and lung. Methylated arsenic species are excreted much faster than inorganic species [15]. The predominant metabolite of inorganic arsenic, dimethylarsinic acid, is rapidly excreted by most mammals. Methylation of inorganic arsenic has been considered to be a detoxification mechanism [16]. It has been suggested that arsenic metabolism and epigenetic changes such as DNA methylation occurring during its metabolism are very important in understanding carcinogenesis and anticancer effects of arsenic [9].

3. Arsenic-induced toxicity

Arsenic causes a variety of adverse health effects such as dermal changes (pigmentation, hyperkeratosis, and ulceration), as well as respiratory, pulmonary, cardiovascular,

gastrointestinal, hematological, hepatic, renal, neurological, developmental, reproductive, immunological, genotoxic, mutagenic, and carcinogenic effects [1]. Many mechanistic studies on arsenic toxicity have suggested that toxicity arising from exposure to arsenic is because of oxidative stress and genotoxicity [17]. Experimental results generated from both *in vitro* and *in vivo* studies of arsenic exposure have suggested that reactive oxygen species (ROS) and reactive nitrogen species are generated during arsenic metabolism [13, 17, 18]. Increased production of reactive oxygen species is induced by arsenic in various human cells such as keratinocytes, vascular smooth muscle cells, and liver cells [19–21]. Toxicity caused by arsenic–induced oxidative stress has also been observed in animal studies. Oxidative stress impairs male reproductive function in mice as demonstrated by a decrease in the testicular GSH level and an increase in the testicular level of protein carbonyls [22]. *In vitro* studies on human fibroblasts, leukocytes, and lymphocytes and hamster embryo cells have shown that arsenic induces genotoxicity including chromosomal aberrations and sister chromatid exchanges [23].

4. Carcinogenesis

The evidence for the carcinogenic effects of arsenic compounds on humans has been based on epidemiological data,

but the exact molecular mechanism of carcinogenesis caused by arsenic is still under investigation by many researchers [24]. Currently accepted molecular mechanisms of arsenic toxicity involve genetic and epigenetic changes, the role of oxidative stress, enhanced cell proliferation and modulation of gene expression.

4.1. *In vitro* studies

Numerous carcinogenic effects have been shown by mammalian cells after exposure to arsenic. Thus, arsenic alters cytosine methylation patterns of the p53 tumor suppressor gene promoter in human lung cells [25]. Cell transformation and cytogenetic effects, including endoreduplication, chromosome aberrations, and sister chromatid exchanges were induced by arsenic in Syrian hamster embryo cells [26]. The inorganic compounds, sodium arsenite and sodium arsenate, were also genotoxic, and tetramethylarsonium iodide and tetraphenylarsonium chloride induced significant increases in the tail moment, reflecting DNA damage, in the TK6 human lymphoblastoid cell line [27]. Kato et al. reported that a 12-h treatment with DMA at 10 mM concentration induced DNA single-strand breaks and DNA-protein crosslinks in L-132 cells, an established human embryonic cell line of type II alveolar cells [28]. Oxidative stress has been postulated to be a

as a mode of arsenic carcinogenicity [29]. Arsenite induced apoptosis in Chinese hamster ovary cells by generating reactive oxygen species [30]. Arsenic induced ROS generation has been reported in various cellular systems, including mouse epidermis-derived cells, human leukemic monocyte lymphoma cells, human aortic smooth muscle cells, human acute promyelocytic leukemia-derived cells, and bovine aortic endothelial cells [20, 30-35]. The reaction and interaction of the reactive species with target molecules is considered to induce oxidative stress, DNA damage, and activation of signaling cascades associated with tumor promotion and/or progression [17].

4.2. *In vivo* studies

Various arsenic compounds have been tested for carcinogenicity by subcutaneous injection, oral intubation, and inhalation of dust and fumes [1, 36, 37]. Although there is still no evidence that tumors are directly induced by exposure to arsenic, animal studies have recently shown that arsenic can cause cancer in mice or contribute to the development of urinary bladder, liver, and lung cancer in adult offspring [38, 39]. DMA, when administered at high doses in the diet for two years, has been shown to induce bladder tumors in rats [40]. Wei et al. [41] also tested DMA as a complete carcinogen and

found it to be carcinogenic to the rat urinary bladder. The urinary system is a more sensitive target for DMA than MMAV [13]. MMAV, however, induced a thickened wall, edema, and hemorrhagic, necrotic, ulcerated, or perforated mucosa in the large intestine and a significant increase in the incidence of squamous metaplasia of epithelial columnar absorptive cells in the colon and rectum [42, 43]. When pregnant mice were treated with arsenic through drinking water, multi-tissue tumorigenesis was observed in the adult offspring. Male C3H mice, exposed to arsenic in utero developed liver carcinoma and adrenal cortical adenoma during adulthood. Female C3H offspring showed dose-related increases in ovarian tumors and lung carcinoma and in proliferative lesions of the uterus and oviducts [38, 39]. Male CD1 mice treated with arsenic in utero developed tumors of the liver and adrenal and kidney hyperplasia, whereas female mice developed tumors of the urogenital system, including the ovaries and uterus, and of the adrenal gland, and hyperplasia of the oviduct [44, 45]. Rudnay and Borzsonyi [46] reported lung adenoma in offspring mice and Pershagen et al. [47] reported low incidences of carcinomas, adenomas, papillomas and adenomatoid lesions of the respiratory tract in hamsters after they were administered arsenic by intratracheal instillation once weekly for 15 weeks.

5. Anticancer activity

ATO is considered to promote differentiation and to induce apoptosis in cancer cells as well as normal cells by modulating redox balance and/or mitochondrial membrane potential loss [17-18]. Considering that one mechanism of carcinogenesis is the inability to execute apoptotic cell death in premalignant stages, this agents could be extremely useful for inducing apoptosis in premalignant cells directly and/or changing the biological background so as to cause the apoptotic death of cancer cells indirectly. Therefore, arsenic compounds have been used for medical purposes [10]. ATO can induce clinical remission in patients with APL via induction of differentiation and programmed cell death. This anti-cancer activity of ATO is not limited to APL, but has also been demonstrated against many solid tumors, including those of the liver, cervix, prostate, lung, esophagus, and bladder [48-53]. However, ATO appears to not be as effective against solid tumors as against APL because high ATO doses are required to induce noticeable anti-cancer effects on solid tumors.

5.1. *In vitro studies*

An *in vitro* study has shown that a high concentration of ATO inhibits growth and promotes apoptosis in many different

cancer cell lines, including colon, liver, gut, lung, prostate and kidney cancer cells [49, 50, 54-59]. Arsenic reduced proliferation and induced apoptosis of hepatoma-derived cells, such as SK-Hep-1, HepG2, and HuH7 [58], and G2/M phase arrest of gastric cancer cells [60]. ATO also induced apoptosis in the colon cancer cell line SW480 by activation of caspase-3 [57]. ATO reduces the invasive and metastatic properties of cervical cancer cells *in vitro* and *in vivo* [53]. Incubation of human umbilical vein endothelial cells with ATO prevented capillary tubule and branch formation in an *in vitro* endothelial cell differentiation assay [61].

5.2. *In vivo* studies

Majority of the evidence has suggested that arsenic has anticancer effects on solid tumors in laboratory animals. Intratumoral delivery of ATO efficiently suppressed growth of heterotransplanted esophageal carcinoma cells without systemic side effects in severe combined immunodeficient mice [48]. ATO, when administered either intravenously or intratumorally, significantly inhibited tumor growth of the inoculated human hepatocellular carcinoma (HCC) cell line HuH7 in a murine xenograft model [62] and also inhibited growth of HCC tumors in mice and growth of human gastric cancer cells subcutaneously implanted in nude mice [63, 64].

Low doses of ATO could delay solid tumor growth by depleting regulatory T cells through oxidative and nitrosative bursts in a murine model of colon cancer [65] and local injections of ATO in mycosis fungoides tumor-bearing mice resulted in tumor regression [66].

6. Conclusion

In summary, as illustrated by the variety of *in vitro* and *in vivo* models, increasing evidence suggests that arsenic has roles as a carcinogen or as a chemotherapeutic agent. Much of our knowledge about the effects of arsenic has been inferred from indirect epidemiological and experimental observations. These paradoxical effects of arsenic do not only result from direct or indirect influences on the genetic and epigenetic levels, but are also closely related to the arsenic species, metabolism and length and dose of exposure. A critical issue is the elucidation and understanding of the molecular mechanisms for activation of specific signaling pathways determining whether exposure to arsenic will induce carcinogenic or anti-carcinogenic effects. In present studies, we examined the global protein expression in liver tissues of the cynomolgus monkey and in human hepatoma cells treated with arsenite. Furthermore, we examined the signaling pathway of asrenic-induced alteration of specific enzyme expression, including kinase and

phosphatase, to elucidate the mechanisms underlying arsenic-induced toxicity.

7. References

[1] Mandal BK, Suzuki KT. Arsenic round the world: a review. Talanta 2002; 58: 201-235.

[2] Sullivan RJ. National Air Pollution Control Administration Publication No. APTD 1969; 69: 26-60.

[3] Nriagu JO, Azcue JM, in: J.O. Nriagu (Ed.), Arsenic in the Environment. Part 1: Cycling and Characterization, John Wiley and Sons, Inc, New York, 1990: 1-15.

[4] Jomova K, Jenisova Z, Feszterova M, Baros S, Liska J, Hudecova D, Valko M. Arsenic: toxicity, oxidative stress and human disease. J Appl Toxicol 2011; 31: 95-107.

[5] Orloff K, Mistry K, Metcalf, S. Biomonitoring for environmental exposures to arsenic. J Toxicol Environ Health B Crit Rev 2009; 12: 509-524.

[6] Bhattacharya R, Chatterjee D, Nath B, Jana J, Jacks G, Vahter M. High arsenic groundwater: mobilization, metabolism

and mitigation – an overview in the Bengal delta plain. Mol Cell Biochem 2003; 253: 347–355.

[7] Chowdhury UK, Biswas BK, Chowdhury TR, Samanta G, Mandal BK, Basu GC, Chanda CR, Lodh D, Saha KC, Mukherjee SK, Roy S, Kabir S, Quamruzzaman Q, Chakraborti D. Groundwater arenic contamination in Bangladesh and West Bengal. India Environ Health Perspect 2000; 108: 393–397.

[8] Nickson R, McArthur J, Burgess W, Ahmed KM, Ravenscroft P, Rahmann M. Arsenic poisoning of Bangladesh groundwater. Nature 1998; 395(6700): 338–338.

[9] Cui X, Kobayashi Y, Akashi M, Okayasu R. Metabolism and the paradoxical effects of arsenic: carcinogenesis and anticancer. Curr Med Chem 2008; 15: 2293–2304.

[10] Shen ZX, Chen GQ, Ni JH, Li XS, Xiong SM, Qiu QY, Zhu J, Tang W, Sun GL, Yang KQ, Chen Y, Zhou L, Fang ZW, Wang YT, Ma J, Zhang P, Zhang TD, Chen SJ, Chen Z, Wang ZY. Use of arsenic trioxide (As2O3) in the treatment of acute promyelocytic leukemia (APL): II. Clinical efficacy and pharmacokinetics in relapsed patients. Blood 1997; 89: 3354–3360.

[11] Bode AM, Dong Z. The paradox of arsenic: molecular mechanisms of cell transformation and chemotherapeutic effects. Crit Rev Oncol Hematol 2002; 42: 5-24.

[12] Vahter M. Genetic polymorphism in the biotransformation of inorganic arsenic and its role in toxicity. Toxicol Lett 2000; 112-113: 209-217.

[13] Cohen SM, Arnold LL, Eldan M, Lewis AS, Beck BD. Methylated arsenicals: the implications of metabolism and carcinogenicity studies in rodents to human risk assessment. Crit Rev Toxicol 2006; 36: 99-133.

[14] Sampayo-Reyes A, Zakharyan RA, Healy SM, Aposhian HV. Monomethylarsonic acid reductase and monomethyl arsonous acid in hamster tissue. Chem Res Toxicol 2000; 13: 1181-1186.

[15] Marafante E, Vahter M, Norin H, Envall J, Sandstrom M, Christakopoulos A, Ryhage R, Biotransformation of dimethylarsinic acid in mouse, hamster and man. J Appl Toxicol 1987; 7: 111-117.

[16] Aposhian HV. Enzymatic methylation of arsenic species and other new approaches to arsenic toxicity. Annu Rev

Pharmacol Toxicol 1997; 37: 397-419.

[17] Shi H, Shi X, Liu KJ. Oxidative mechanism of arsenic toxicity and carcinogenesis. Mol Cell Biochem 2004; 255: 67-78.

[18] Yamanaka K, Kato K, Mizoi M, An Y, Takabayashi F, Nakano M, Hoshino M, Okada S. The role of active arsenic species produced by metabolic reduction of dimethylarsinic acid in genotoxicity and tumorigenesis. Toxicol Appl Pharmacol 2004; 198: 385-393.

[19] Cooper KL, Liu KJ, Hudson LG. Contributions of reactive oxygen species and mitogen-activated protein kinase signaling in arsenite-stimulated hemeoxygenase- 1 production. Toxicol Appl Pharmacol 2007; 218: 119-127.

[20] Lynn S, Gurr JR, Lai HT, Jan KY: NADH oxidase activation is involved in arsenite-induced oxidative DNA damage in human vascular smooth muscle cells. Circ Res 2000; 86: 514-519.

[21] Wang Y, Xu Y, Wang H, Xue P, Li X, Li B, Zheng Q, Sun G. Arsenic induces mitochondria-dependent apoptosis by reactive oxygen species generation rather than glutathione depletion in

Chang human hepatocytes. Arch Toxicol 2009; 83: 899-908.

[22] Chang SI, Jin B, Youn P, Park C, Park JD, Ryu DY. Arsenicinduced toxicity and the protective role of ascorbic acid in mouse testis. Toxicol Appl Pharmacol 2007; 218: 196-203.

[23] Helleday T, Nilsson R, Jenssen D. Arsenic and heavy metal ions induce intrachromosomal homologous recombination in the hprt gene V79 Chinese hamster cells. Environ Mol Mutagen 2000; 35: 114-122.

[24] Wang JP, Qi L, Moore MR, Ng JC. A review of animal models for the study of arsenic carcinogenesis. Toxicol Lett 2002; 133: 17-31.

[25] Mass MJ, Wang L. Arsenic alters cytosine methylation patterns of the promoter of the tumor suppressor gene p53 in human lung cells: a model for a mechanism of carcinogenesis. Mutat Res 1997; 386: 263-277.

[26] Lee TC, Oshimura M, Barrett JC. Comparison of arsenic-induced cell transformation, cytotoxicity, mutation and cytogenetic effects in Syrian hamster embryo cells in culture. Carcinogenesis 1985; 6: 1421-1426.

[27] Guillamet E, Creus A, Ponti J, Sabbioni E, Fortaner S, Marcos R. *In vitro* DNA damage by arsenic compounds in a human lymphoblastoid cell line (TK6) assessed by the alkaline Comet assay. Mutagenesis 2004; 19: 129-135.

[28] Kato K, Hayashi H, Hasegawa A, Yamanaka K, Okada S. DNA damage induced in cultured human alveolar (L-132) cells by exposure to dimethylarsinic acid. Environ Health Perspect. 1994; 102 Suppl 3: 285-288.

[29] Kitchin KT. Recent advances in arsenic carcinogenesis: modes of action, animal model systems, and methylated arsenic metabolites. Toxicol Appl Pharmacol 2001; 172: 249-261.

[30] Wang TS, Kuo CF, Jan KY, Huang H: Arsenite induces apoptosis in Chinese hamster ovary cells by generation of reactive oxygen species. J Cell Physiol 1996; 169: 256-268.

[31] Barchowsky A, Klei LR, Dudek EJ, Swartz HM, James PE: Stimulation of reactive oxygen, but not reactive nitrogen species, in vascular endothelial cells exposed to low levels of arsenite. Free Radic Biol Med 1999; 27: 1405-1412.

[32] Corsini E, Asti L, Viviani B, Marinovich M, Galli CL: Sodium arsenate induces overproduction of interleukin-1alpha

in murine keratinocytes: Role of mitochondria. J Invest Dermatol 1999; 113: 760-765.

[33] Iwama K, Nakajo S, Aiuchi T, Nakaya K: Apoptosis induced by arsenic trioxide in leukemia U937 cells is dependent on activation of p38, inactivation of ERK and the Ca2+-dependent production of superoxide. Inter J Cancer 2001; 92: 518-526.

[34] Jing Y, Dai J, Chalmers-Redman RM, Tatton WG, Waxman S: Arsenic trioxide selectively induces acute promyelocytic leukemia cell apoptosis via a hydrogen peroxide-dependent pathway. Blood 1999; 94: 2102-2111.

[35] Liu F, Jan KY: DNA damage in arsenite- and cadmium-treated bovine aortic endothelial cells. Free Radic Biol Med 2000; 28: 55-63.

[36] International Agency for Research on Cancer (IARC). Evaluation of Carcinogenic Risks to Humans. 1987; Suppl. 7: 100.

[37] International Agency for Research on Cancer (IARC). IARC Monograph on Evaluation of Carcinogenic Risk to Humans. 1980; Suppl. 23: 39.

[38] Waalkes MP, Liu J, Ward JM, Diwan BA. Animal models for arsenic carcinogenesis: inorganic arsenic is a transplacental carcinogen in mice. Toxicol Appl Pharmacol 2004; 198: 377-384.

[39] Waalkes MP, Ward JM, Diwan BA. Induction of tumors of the liver, lung, ovary and adrenal in adult mice after brief maternal gestational exposure to inorganic arsenic: promotional effects of postnatal phorbol ester exposure on hepatic and pulmonary, but not dermal cancers. Carcinogenesis 2004; 25: 133-141.

[40] Gemert M, Eldan M. Chronic carcinogenicity assessment of cacodylic acid. In Society for Environmental Geochemistry and Health (SEGH) Third International Conference on Arsenic Exposure and Health Effects, Book of Abstracts, San Diego, CA, 1998; 12-15: 113.

[41] Wei Li, Wanibuchi H, Salim EI, Yamamoto S, Yoshida K, Endo G, Fukushima S. Promotion of NCIBlack- Reiter male rat bladder carcinogenesis by dimethylarsinic acid an organic arsenic compound. Cancer Lett 1998; 134: 29-36.

[42] Arnold LL, Eldan M, van Gemert M, Capen CC, Cohen SM.

Chronic studies evaluating the carcinogenicity of monomethylarsonic acid in rats and mice. Toxicology 2003; 190: 197-219.

[43] Gur E, Pirak M, Waner T. Methanearsonic acid oncogenicity study in the mouse. Luxembourg Industries (Pamol) Ltd. Submitted to the US Environmental Protection Agency. 1991.

[44] Waalkes MP, Liu J, Ward JM, Diwan BA. Enhanced urinary bladder and liver carcinogenesis in male CD1 mice exposed to transplacental inorganic arsenic and postnatal diethylstilbestrol or tamoxifen. Toxicol Appl Pharmacol 2006; 215: 295-305.

[45] Waalkes MP, Liu J, Ward JM, Powell DA, Diwan BA. Urogenital carcinogenesis in female CD1 mice induced by in utero arsenic exposure is exacerbated by postnatal diethylstilbestrol treatment. Cancer Res 2006; 66: 1337-1345.

[46] Rudnay P, Borzsonyi M. The tumorigenic effect of treatment with arsenic trioxide (Hung). Magyar Onkol 1981; 25: 73-77.

[47] Pershagen G, Nordberg G, Bjorklund NE. Carcinomas of the respiratory tract in hamsters given arsenic trioxide and/or

benzo(a)pyrene by the pulmonary route. Environ Res 1984; 34: 227-241.

[48] Diepart C, Karroum O, Magat J, Feron O, Verrax J, Calderon PB, Grégoire V, Leveque P, Stockis J, Dauguet N, Jordan BF, Gallez B. Arsenic trioxide treatment decreases the oxygen consumption rate of tumor cells and radiosensitizes solid tumors. Cancer Res 2012; 72: 482-490.

[49] Maeda H, Hori S, Nishitoh H, Ichijo H, Ogawa O, Kakehi Y, Kakizuka A. Tumor growth inhibition by arsenic trioxide (As2O3) in the orthotopic metastasis model of androgen-independent prostate cancer. Cancer Res 2001; 61: 5432-5440.

[50] Murgo AJ. Clinical trials of arsenic trioxide in hematologic and solid tumors: overview of the National Cancer Institute Cooperative Research and Development Studies. Oncologist 2001; 2: 22-28.

[51] Shen ZY, Zhang Y, Chen JY, Chen MH, Shen J, Luo WH, Zeng Y. Intratumoral injection of arsenic to enhance antitumor efficacy in human esophageal carcinoma cell xenografts. Oncology reports 2004; 11: 155-159.

[52] Yu J, Qian H, Li Y, Wang Y, Zhang X, Liang X, Fu M, Lin C.

Arsenic trioxide (As2O3) reduces the invasive and metastatic properties of cervical cancer cells *in vitro* and *in vivo*. Gynecol Oncol 2007; 106: 400-406.

[53] Yu J, Qian H, Li Y, Wang Y, Zhang X, Liang X, Fu M, Lin C. Therapeutic effect of arsenic trioxide (As2O3) on cervical cancer *in vitro* and *in vivo* through apoptosis induction. Cancer Biol Ther 2007; 6: 580-586.

[54] Hyun Park W, Hee Cho Y, Won Jung C, Oh Park J, Kim K, Hyuck Im Y, Lee MH, Ki Kang W, Park K. Arsenic trioxide inhibits the growth of A498 renal cell carcinoma cells via cell cycle arrest or apoptosis. Biochem Biophys Res Commun 2003; 300: 230-235.

[55] Jin HO, Yoon SI, Seo SK, Lee HC, Woo SH, Yoo DH, Lee SJ, Choe TB, An S, Kwon TJ, Kim JI, Park MJ, Hong SI, Park IC, Rhee CH. Synergistic induction of apoptosis by sulindac and arsenic trioxide in human lung cancer A549 cells via reactive oxygen species-dependent down-regulation of survivin. Biochem Pharmacol 2006; 72: 1228-1236.

[56] Kim HR, Kim EJ, Yang SH, Jeong ET, Park C, Kim SJ, Youn MJ, So HS, Park R. Combination treatment with arsenic trioxide and sulindac augments their apoptotic potential in lung

cancer cells through activation of caspase cascade and mitochondrial dysfunction. Int J Oncol 2006; 28: 1401-1408.

[57] Nakagawa Y, Akao Y, Morikawa H, Hirata I, Katsu K, Naoe T, Yagi K. Arsenic trioxide-induced apoptosis through oxidative stress in cells of colon cancer cell lines. Life sciences 2002; 70: 2253-2269.

[58] Oketani M, Kohara K, Tuvdendorj D, Ishitsuka K, Komorizono Y, Ishibashi K, Arima T. Inhibition by arsenic trioxide of human hepatoma cell growth. Cancer letters 2002; 183: 147-153.

[59] Zhang TC, Cao EH, Li JF, Ma W, Qin JF. Induction of apoptosis and inhibition of human gastric cancer MGC-803 cell growth by arsenic trioxide. Eur J Cancer 1999; 35: 1258-1263.

[60] Li Y, Qu X, Qu J, Zhang Y, Liu J, Teng Y, Hu X, Hou K, Liu Y. Arsenic trioxide induces apoptosis and G2/M phase arrest by inducing Cbl to inhibit PI3K/Akt signaling and thereby regulate p53 activation. Cancer Lett 2009; 284: 208-215.

[61] Roboz GJ, Dias S, Lam G, Lane WJ, Soignet SL, Warrell Jr RP, Rafii S. Arsenic trioxide induces dose-and time-dependent apoptosis of endothelium and may exert an antileukemic effect

via inhibition of angiogenesis. Blood 2000; 96: 1525-1530.

[62] Kito M, Matsumoto K, Wada N, Sera K, Futatsugawa S, Naoe T, Nozawa Y, Akao Y. Antitumor effect of arsenic trioxide in murine xenograft model. Cancer Sci 2003; 94: 1010-1014.

[63] Liu B, Pan S, Dong X, Qiao H, Jiang H, Krissansen GW, Sun X. Opposing effects of arsenic trioxide on hepatocellular carcinomas in mice. Cancer science 2006; 97: 675-681.

[64] Wu DD, Xiao YF, Geng Y, Hou J. Antitumor effect and mechanisms of arsenic trioxide on subcutaneously implanted human gastric cancer in nude mice. Cancer Genet Cytogenet 2010; 198: 90-96.

[65] Thomas-Schoemann, A., Batteux F, Mongaret C, Nicco C, Chéreau C, Annereau M, Dauphin A, Goldwasser F, Weill B, Lemare F, Alexandre J. Arsenic trioxide exerts antitumor activity through regulatory T cell depletion mediated by oxidative stress in a murine model of colon cancer. J Immunol 2012; 189: 5171-5177.

[66] Tun-Kyi A, Qin JZ, Oberholzer PA, Navarini AA, Hassel JC, Dummer R, Döbbeling U. Arsenic trioxide down-regulates

antiapoptotic genes and induces cell death in mycosis fungoides tumors in a mouse model. Ann Oncology 2008; 19: 1488-1494.

CHAPTER Ⅰ

ARSENITE-INDUCED CHANGES IN HEPATIC PROTEIN ABUNDANCE IN CYNOMOLGUS MONKEYS (*MACACA FASCICULARIS*)

1. Introduction

Arsenic has been associated with cancers of the skin, bladder, lung, kidney, and liver as well as with noncancerous conditions, such as diabetes and hepatopathy [1–5]. Some studies suggest that toxicity arising from exposure to arsenic is due to oxidative stress and genotoxicity. Increased production of reactive oxygen species is induced by arsenic in various human cells such as keratinocytes [6], vascular smooth muscle cells [7], and liver cells [8]. Depletion of glutathione (GSH) and antioxidant enzymes such as glutathione peroxidase (GPx) is also noted in arsenictreated hepatoma cells [9]. Toxicity caused by arsenic-induced oxidative stress has also been observed in animal studies. Induction of oxidative stress in mice impairs male reproductive function as evidenced by a decrease in the testicular GSH level and an increase in the testicular level of protein carbonyl [10]. Arsenic treatment decreases hepatic activities of oxidative stress related enzymes such as catalase, GPx, glutathione reductase (GR), and glucose-6-phosphate dehydrogenase (G6PD) in rats, but the effect of arsenic is alleviated by treatment of metal-chelating antioxidants [11, 12]. GR and G6PD do not act on ROS directly, but enable GPx to function [13]. GPx-1 is an intracellular antioxidant enzyme that uses GSH as an obligate cosubstrate in the reduction of hydrogen peroxide to water [14]. Catalase also

converts hydrogen peroxide into water. Chk2 is activated through the phosphorylation of Thr68 in response to DNA damage, triggering cell-cycle arrest or apoptosis via p53, and other effector molecules [15, 16]. Histone H2AX phosphorylation, producing _-H2AX, leads to the recruitment of molecules of the repair machinery at the site of DNA damage [17]. Proliferative cell nuclear antigen (PCNA) increases the processivity of DNA synthesis [18], and is involved in a variety of DNA metabolism processes [19]. Monoubiquitination of PCNA leads to the recruitment of several damage-tolerant DNA polymerases at the site of DNA damage [20, 21]. The p53 protein is stabilized and accumulates in response to DNA damage signals. Arsenic induces p53 protein expression in several human cell types [22, 23]. Exposure to arsenic is associated with alterations in glucose homeostasis, as demonstrated in many animal studies [24–27]. Arsenite treatment causes a decrease in blood glucose levels in rats [25] and in mice-fed high-fat diets [26]. Furthermore, arsenic trioxide inhibits hepatic gluconeogenesis in rats [27]. Hepatic gluconeogenesis is mainly mediated sequentially by pyruvate carboxylase (PCB), phosphoenolpyruvate carboxykinase (PEPCK), fructose-1,6-bisphosphatase (FBPase), and glucose-6-phosphatase (G6Pase). Among them, two of the rate-limiting step enzymes that play a central role in gluconeogenesis are FBPase [28] and PEPCK, which catalyzes

the first committed step in gluconeogenesis [29].

In the present study, we examined the global protein expression in liver tissues of cynomolgus monkeys orally administered with sodium arsenite (SA) for 28 days to elucidate the mechanisms underlying inorganic arsenic induced liver toxicity. We identified proteins differentially expressed in monkey livers after treatment with SA using 2D-PAGE and MS analysis, and validated the data by Western blot and immunohistochemistry (IHC) for four selected proteins. Proteins related to arsenic-induced toxicity, such as oxidative stress related, genotoxicity-related, and glucose metabolism related proteins, were also analyzed inmonkey livers. In addition, differential expression of the proteins studied inmonkey tissues was also assessed in human hepatoma cells treated with SA.

2. Material and methods

2.1. Chemicals

All chemicals used in this study were of reagent grade or higher, and were obtained from Sigma-Aldrich (St. Louis, MO), unless otherwise specified.

2.2. Animal treatment

All animals in this study were used in accordance with the principles outlined in the “Guide for the Care and Use of Laboratory Animals” (National Institutes of Health). The experimental protocol for animal use in this study was approved by the Institutional Animal Care and Use Committee of Korea Institute of Toxicology (Daejun, South Korea; approval #20080506). Six male cynomolgus monkeys (Macaca fascicularis) were purchased from Hamri Co. Ltd (Ibaraki, Japan) at three to six years of age, and were quarantined at the nonhuman primate facility at Korea Institute of Toxicology for 30 days, during which they were subjected to various physical examinations, a tuberculosis test, and microbiological tests for Salmonella, Shigella, and Yersinia. Then, the monkeys were acclimated for 28 days before initial dosing. The animals were housed individually in stainless steel wire cages (543 W × 715 L × 818 H mm) and provided a standard monkey diet (Oriental Yeast Co., Tokyo, Japan) and filtered tap water ad libitum. The animal room was maintained at a temperature of 23 ± 3 ℃, relative humidity of 55 ± 10%, air ventilation of 10–20 times/h, and a light intensity of 150–300 Lux with a 12 h light/dark cycle. The body weights of the animals ranged from 3.5 to 4.5 kg at commencement of dosing. The monkeys were randomly divided

into two groups, with three monkeys assigned per group. The animals in the treatment group were orally administrated using an oral sonde with water containing 1.73 mg/kg/day SA (1.0 mg/kg/day arsenic) at a volume of 5mL/kg, while animals in the control group were given plain water. On the 28th day of treatment, the monkeys were euthanized with an overdose of sodium pentothal. Liver tissues were collected, frozen immediately in liquid nitrogen, and stored in a deep freezer. Portions of liver tissues were fixed in 10% formalin, embedded in paraffin, sectioned, andmounted on slides for histological examination.

2.3. 2D-PAGE

For total protein extraction, liver tissues were minced and suspended in sample buffer containing 40 mM Tris, 7 M urea, 2Mthiourea, 4.5% CHAPS, 100 mM1,4-dithioerythritol, and a protease inhibitor cocktail (Roche, Mannheim, Germany). Suspensions were sonicated and centrifuged at 100,000 × g for 45 min. The clarified sample (1 mg of protein) was applied to immobilized pH 3–10 nonlinear gradient strips (Amersharm Biosciences, Uppsala, Sweden), and IEF was performed at 80 000 Vh [30]. For second dimension separation, electrophoresis was performed in 9–16% linear gradient polyacrylamide gels (18 cm × 20 cm × 1.5 mm) at a constant current of 40 mA

per gel for approximately 5 h. After protein fixation in 40% methanol and 5% phosphoric acid for 1 h, the gels were stained with CBB G250 (Bio-Rad,Hercules, CA). Stained gels were scanned using a GS-710 Imaging Densitometer (Bio-Rad) and analyzed with an Image Master Platinum 5 program (GE Healthcare, Milwaukee, WI).

2.4. MS

Protein spots were excised from gels with a sterile scalpel and were digested using trypsin (Promega, Madison, WI) [31]. For MALDI-TOF MS analysis, the tryptic peptides were washed with a POROS R2/Oligo R3 resin column (Applied Biosystems, Foster City, CA) and eluted with cyano- 4-hydroxycinamic acid dissolved in 70% ACN and 2% formic acid before MALDI-TOF MS analysis [32]. Mass spectra were acquired on a 4800 Proteomics Analyzer (Applied Biosystems) operated in MS and MS/MS modes. Peptide fragmentation in MS/MS mode was by collision-induced dissociation using atmosphere as the collision gas. The instrument was operated in reflectron mode and calibrated using the 4800 calibration mixture (Applied Biosystems); each sample spectrum was additionally calibrated using trypsin autolysis peaks. Peptide mass fingerprinting was performed using the Mascot search engine (http://www.matrixscience.com). Peptide matching and

protein searches were performed using Swiss-Prot and NCBI databases.

2.5. Cell treatment

The human hepatoma HepG2 cell line was grown in RPMI-1640 medium containing 2mg/mL sodium bicarbonate, 10% (v/v) FBS, 100 units/mL penicillin, and 100 mg/mL streptomycin. The cells were maintained at 37℃ in a 5% CO2 incubator. Then, 24 h after the cells were plated, the culture medium was removed and replaced with medium containing various concentrations of SA. After 24 h of SA exposure, the cells were harvested for Western blotting. In addition, 3-(4,5-dimethylthiazol-2-yl)-2,5-diphenyltetrazolium bromide (MTT) reduction was used to assess cell viability.

2.6. Western blot

Sample preparation and Western blotting were performed as previously described [33]. Anti-PEPCK 2 (PEPCK-M, sc-130388), anti-PCNA (sc-56), anti-G6Pase (sc-25840), anti-PCB (sc-46228), and anti-FBPase (sc-66946) antibodies were purchased from Santa Cruz Biotechnology (Santa Cruz, CA). Anti-mortalin (ab2799), anti-PEPCK1

(PEPCK-C, ab28455), anti-catalase (ab16731), anti-G6PD (ab87230), and anti-GR (ab16801) antibodies were purchased from Abcam (Cambridge, MA). Anti-selenium-binding protein (SBP1, M061-3) and anti-GPx-1 (GPx-1, M015-3) antibodies were purchased from MBL (Nagoya, Japan). Anti-cystathionine beta-synthase (CBS,H00000875-A01) antibody was purchased fromAbnova (Taipei, Taiwan). Anti-γ-H2AX (P16104) antibody was purchased from Millipore (Billerica, MA). Anti-phospho-Chk2 (p-Chk2, #2197) antibody was purchased from Cell Signaling Technology (Beverly, MA). Anti-p53 (IR616) antibody was purchased from Dako (Cambridge, UK). HRP-conjugated goat anti-mouse IgG (SA001-500),HRP-conjugated goat antirabbit IgG (SA002-500), and HRP-conjugated rabbit anti-goat IgG (SA007-500) were purchased from GenDepot (Barker, TX).

2.7. IHC

Monkey liver tissue sections (5 μm thick) were deparaffinized in xylene, dehydrated in graded ethanol, and rehydrated. For antigen retrieval, sections were heated to boiling point in a stainless steel pressure cooker containing diluted Antigen Unmasking Solution (H3300, Vector Laboratories, Burlingame, CA), according to the manufacturer's protocol. Endogenous peroxidase activity was inhibited with

PBS containing 0.3% hydrogen peroxide for 30 min. After blocking with normal donkey serum for 2 h, tissue sections were incubated with specific primary antibodies diluted in TBS overnight at 4℃. Biotin-labeled anti-mouse or anti-rabbit antibody (BA-2000 or BA-1000, Vector Laboratories), Vectastain Elite ABC kit (PK-6102, Vector Laboratories), and DAB substrate kit (SK-4100, Vector Laboratories) were sequentially used according to the manufacturers' instructions. Sections were counterstained with Mayer's hematoxylin.

2.8. Statistical analysis

The Mann–Whitney test was performed to compare specific protein abundance differences between SA-treated and control-treated monkey groups (SAS 9.13 statistical program, SAS Institute, Cary, NC). Proteins whose abundance differed between the two groups were identified using an empirical criterion of a more than fivefold change in mean spot volume and $p \leq 0.05$. The IC50 value, corresponding to the concentration producing a 50% inhibition of cell viability, was determined by probit analysis (Biostat 2009, AnalystSoft, Vancouver, Canada).

3. Results

More than 1000 protein spots were visualized on 2D-PAGE from liver tissues from six monkeys (SA-treated group, n = 3; control-treated group, n = 3). Among them, 16 protein spots were significantly changed (more than fivefold differences in mean spot volume and p _ 0.05) in SA-treated monkey liver tissues compared to control-treated monkey liver tissues, with increases and decreases in protein levels seen in two and 14 spots, respectively (Figure 1). The stringent criteria was applied in order to reduce the rate of false-positive detection. These spots were then identified by peptide mass fingerprinting based on MS analysis and a database search. The lists of proteins with increased and decreased abundance are summarized in Tables 1 and 2, respectively. MS and MS/MS data are shown in Supporting Information Tables 1 and 2, respectively.

To validate the proteomic data, the abundance of four selected proteins, mortalin, CBS, SBP1, and PEPCK-M, was further analyzed using IHC (Figure 2A) and Western blotting (Figure 2B). The four proteins were selected based upon their potential functional roles in carcinogenesis and glucose metabolism-related diseases (further discussed in the Discussion section). In both analyses, quantitative changes of the four proteins were confirmed, that is, the abundance of

mortalin was higher in SA-treated monkey liver tissues than in control-treated monkey liver tissues, and the protein levels of CBS, SBP1, and PEPCK-M were lower in SA-treated monkey liver tissues than in control-treated monkey liver tissues. These differences validate the proteomic data shown in Tables 1 and 2. IHC for the four proteins showed granular cytoplasmic staining without membranous staining.

Western blotting was used for analysis of the abundance of the four proteins in human hepatoma HepG2 cells treated with three different concentrations of SA (Figure 2B). The highest concentration of SA used in the cellular treatment, 15 μM, was half the IC50 dose based on an MTT assay (data not shown). Similarly to the differential expression levels seen in monkey liver tissues, the level of mortalin increased in HepG2 cells in a dose-dependent manner after 24 h treatment with SA, and the levels of CBS, SBP1, and PEPCK-M all dose dependently decreased in these cells.

In addition, protein levels of oxidative stress related enzymes, including G6PD, GPx-1, catalase, and GR, were analyzed in monkey liver tissues and HepG2 cells (Figure 3). The level of G6PD was higher in SA-treated monkey liver tissues than in control-treated monkey liver tissues. In addition, the level of G6PD dose-dependently increased in HepG2 cells treated with SA for 24 h.

The level of GPx-1 was lower in liver tissues from

monkeys treated with SA- than in those of control-treated monkeys, and decreased in HepG2 cells after 24 h treatment with SA in a dose-dependent manner. In contrast to G6PD and GPx-1, the protein levels of catalase and GR were not affected by SA treatment in monkey liver tissues. The level of GR was also unchanged in SA-treated HepG2 cells; however, the protein level of catalase decreased dose-dependently in SA-treated HepG2 cells.

Genotoxicity is an important mechanism in arsenic induced toxicity. Therefore, we analyzed the protein levels of four DNA damage and metabolism-related proteins: γ- H2AX, PCNA, p-Chk2, and p53 (Figure 4). The protein level of γ-H2AX was higher in SA-treated monkey liver tissues than in control-treated monkey liver tissues and increased in HepG2 cells treated with SA, indicating SA-induced DNA damage. The level of unmodified and modified forms of PCNA was also higher in SA-treated monkey liver tissues than in control-treated monkey liver tissues (Figure 4). Mono-ubiquitinated PCNA, which is related to DNA damage repair, is expected to migrate 5–10 kDa higher than non-ubiquitinated PCNA [34].

The levels of both forms of PCNA increased dose dependently in HepG2 cells following treatment with SA. These data suggest that PCNA-related DNA metabolism processes, such as replication and repair, are activated following SA treatment in liver tissue and hepatic cells. The level of p-Chk2

was dramatically higher in SA-treated monkey liver tissues than in livers of control-treated animals, indicating that the liver undergoes SA-induced DNA damage (Figure 4). However, the level of p53 protein was unchanged after treatment with SA in monkey liver tissues. In addition, neither p-Chk2 nor p53 levels were altered in HepG2 cells following SA treatment.

Based on the decreased levels of PEPCK-M in SA-treated monkey liver tissues and HepG2 cells (Table 2 and Figure 1 and 2), we further investigated other gluconeogenesis-related enzymes: PCB, PEPCK-C, FBPase1, and G6Pase (Figure 5). The expression level of PCB was higher in SA-treated monkey liver tissues than in control-treated monkey liver tissues, and also increased dose-dependently in HepG2 cells following treatment with SA.

In contrast to PCB, the expression level of PEPCK-C was lower in SA-treated monkey livers than in control-treated monkey livers, as was the case for PEPCK-M (Figure 1 and 2, Table 2). The level of PEPCK-C also decreased in HepG2 cells after treatment with SA in a dose-dependent manner, which is comparable to the effect seen for PEPCK-M (Figure 2). In addition, the expression levels of FBPase1 and G6Pase were lower in SA-treated monkey liver tissues than in control treated monkey liver tissues, and dose-dependently decreased in SA-treated HepG2 cells.

4. Discussion

The NOAEL/LOAEL values for arsenic-induced hepatotoxicity range from 0.69 to 25 mg/kg/day in 15–364 day oral administration studies for a variety of non-primate animals [35]. In addition, monkeys have been used to assess arsenic intoxication in several studies. In one study [36], adolescent rhesus monkeys given 7.5 mg/kg/day arsenic trioxide developed vomiting and unformed fecal stools within five days of oral administration of arsenic. Vacuolation of hepatocytes was observed in their livers, showing a marked decrease in glycogen. Another study examined the tissue and subcellular localization of arsenic in marmoset monkeys given 74As-arsenite. The highest tissue accumulation of arsenic at four days after arsenic dosing was found in the liver, with 50% of arsenic bound to rough microsomal fractions [37]. However, Thorgeirsson et al. reported that arsenic did not prove to be carcinogenic in cynomolgus monkeys given sodium arsenate for 15 years at 0.1 mg/kg five times per week [38]. Based upon these studies, It was assumed that the dose level used in this study, 1.73 mg/kg/day SA (1.0 mg/kg/day arsenic), is adequate for 28-day oral administration in monkeys.

With the exception of two proteins, catalase and p-Chk2, the levels of proteins analyzed in this study showed similar trends following arsenic treatment in monkey liver tissue and

human hepatoma cells. (Figure 2–5). In view of the similar regulation of proteins in human cells and in an animal model using monkeys, which are genetically related to humans, our results indicate that these arsenic-induced changes in hepatic protein expression reflect the adverse health effects of arsenic exposure in humans.

Mortalin sequesters the p53 tumor suppressor protein in the cytoplasm to inhibit its function [39, 40]. In addition, the induction of mortalin is considered a marker for hepatocellular carcinoma (HCC) metastasis and recurrence [41]. The level of mortalin is elevated in immortalized human keratinocytes after treatment with arsenite [42]. The present study also demonstrated an increased level of mortalin in the livers of arsenic-treated monkeys (Table 1, Figure 1 and 2).

Reduced plastin-3 expression is associated with induction of apoptosis [43]. Plastin-3 plays a role in controlling cell cycle and DNA damage repair [44, 45]. Overexpression of plastin-3 has been found in cisplatin-resistant [46] and ultraviolet radiation resistant [47] cells. The decreased expression of plastin-3 in monkey livers observed in the current study (Table 2) may render hepatocytesmore sensitive to DNA damage and apoptotic insults.

Similarly to plastin-3, TBK1 is also thought to inhibit apoptosis via TNF-mediated NF-κB activation [48]. In support of these findings, TBK1-deficient mice are

embryonically lethal due to massive liver apoptosis [49]. In the current study, the low expression of TBK1 observed in livers from monkeys treated with SA (Table 2) may contribute to cellular toxicity.

CBS is under tight regulation due to its critical role in antioxidant and methylation metabolism [50]. A genetic variation study showed that CBS may influence methylation metabolism of arsenic and susceptibility to arsenic-related diseases, such as atherosclerosis, in humans [51, 52]. Expression of CBS is downregulated in HCC and is associated with a poor prognosis [53]. In view of these findings, the lower expression of CBS in liver tissues of SA-treated animals versus control-treated animals (Table 2, Figure 1 and 2) may have an impact on the metabolism of arsenic as well as on arsenic induced hepatotoxicity.

Inhibition of SBP1 effectively increases HCC cell motility, promotes HCC cell proliferation, and inhibits oxidative stress induced apoptosis of HCC cells [54]. Levels of SBP1 are lower in various human epithelial cancers, including HCC, than in normal tissues [54, 55]. The downregulation of SBP1 in SA-treated monkey liver tissues (Table 2, Figure 1 and 2) indicates that SBP1 may play a role in the development of hepatotoxicity, including carcinogenesis.

Annexin A6, a Ca^{2+}-dependent phospholipid binding protein [56], is considered to be a tumor suppressor that

reduces the transforming potential of Ras [57, 58]. Annexin A6 is downregulated in several human primary cancers [59]. Thus, the reduced expression level of annexin A6 in SA treated monkey liver tissue compared to that in control treated monkey liver tissue (Table 2) may contribute to carcinogenesis.

Alpha-enolase is a multifunctional enzyme that plays a role in various processes such as glycolysis, growth control, hypoxia tolerance, and immune responses [60]. It is also involved in cellular protection against oxidative stress [61]. Alpha-enolase function is impaired by oxidative damage in human umbilical vein endothelial cells treated with arsenite [62]. The reduced expression of alpha-enolase (Table 2) seen in the current study might play a role in the development of hepatotoxicity.

Downregulation of erlin-2 inhibits degradation of inositol 1,4,5-trisphosphate receptors, leading to pathological changes in Ca2+ signaling causing cellular apoptosis [63]. The decreased expression of erlin-2 in the current study (Table 2) might contribute to the susceptibility of liver cells to cellular toxicity.

The catabolism of arginine may be disturbed in hepatic cells due to the decreased expression of arginase-1 in monkey liver tissues (Table 2). Arginine is a precursor for the synthesis of nitric oxide (NO), and arginase and NO synthase may compete for arginine as a substrate. Excessive cellular NO

is associated with many important pathological processes, such as carcinogenesis and tumor progression [64]. In a previous study, the expression of arginase-1 was lower in HCC than in normal liver tissue [65]. The downregulation of arginase-1 seen in the current study might be a risk factor for hepatotoxicity following SA exposure.

In the present study, however, the expression levels of two oxidative stress related enzymes, G6PD and GPx-1, were altered by arsenic treatment in monkey livers, but showed changes in opposing directions (Figure 3). Modulation of cellular G6PD activity represents an important component of the integrated response to external stimuli such as oxidative stress [66]. Hence, the elevated expression of G6PD in monkey livers following SA treatment may be a result of the cellular adaptive and defensive regulation exerted against arsenic-induced oxidative damages. However, a few recent studies have suggested that an abnormal increase in G6PD may be detrimental to beta cells and macrophages [67, 68].

GPx-1 is transcriptionally upregulated in response to oxidative stress, and paraquat, a redox cycler, stimulates GPx-1 promoter activity [69]. Surprisingly, the expression levels of GPx-1 were decreased in SA-treated monkey livers and hepatoma cells (Figure 3). The decrease in GPx-1 protein expression levels might contribute to arsenic-induced hepatotoxicity.

In the current study, activation of DNA damage related proteins following SA exposure was shown by the ubiquitination of PCNA and the phosphorylation of H2AX and Chk2 (Figure 4). This supports the previous notion that arsenic induced DNA damage, in addition to arsenic-induced cellular signaling changes and oxidative stress, plays an important role in arsenic-induced toxicity [70, 71]. Enhanced expression of PCNA may indicate arsenic-induced enhancement of hepatic cell proliferation [19].

Hepatic gluconeogenesis occurs during prolonged fasting episodes and begins with the induction of PCB when acetyl-CoA is abundant. In the present study, the expression level of PCB was increased in arsenic-treated monkey livers, while the expression levels of downstream enzymes such as PEPCK-M, PEPCK-C, FBPase1, and G6Pase were decreased (Table 2, Figure 1, 2, and 5). Based on the reduced expression of rate-limiting enzymes such as PEPCK and FBPase1, glucose production by gluconeogenesis was likely to be severely inhibited in arsenic-treated monkey livers. These data are in agreement with previous studies in which the expression of PEPCK [72-74] and G6Pase [73] is inhibited by arsenite in hepatic cells. Arsenite also inhibits G6Pase activity in liver tissues of rats [25]. Our data, in addition to these previous reports, strongly suggest that arsenic perturbs glucose metabolism, which may ultimately lead to carbohydrate

metabolism-related diseases in arsenic-exposed individuals.

Insulin controls hepatic glucose production through the regulation of glycogen metabolism and gluconeogenesis; the regulation of the latter is dependent on the gene expression levels of PEPCK and G6Pase [75]. While PEPCK and G6Pase are primarily regulated at the transcriptional level [76], the activity of FBPase is mainly modulated by negative effectors such as fructose-2,6-bisphosphate and adenosine monophosphate, and by its interaction with fructose 1,6-bisphosphate aldolase [77, 78]. Mutual downregulation of PEPCK, FBPase, and G6Pase expression has been observed in important mouse and hepatic diseases such as mouse nonalcoholic hepatitis and HCC as well as human HCC [79]. Agonists for liver X-activated receptors, which are important regulators of cholesterol, fatty acid, and glucose homeostasis, also suppress the expression of PEPCK, FBPase, and G6Pase [80, 81].

Taken together, subchronic treatment of inorganic arsenic in cynomolgus monkeys modified the expression levels of a variety of hepatic proteins. In view of the reported functions of these proteins, the changes in expression levels of certain liver proteins may contribute to arsenic-induced hepatotoxicity, while the modulation of other proteins may reflect the activation of protective and adaptive mechanisms toward arsenic-induced toxicity. Interestingly, many of the differentially expressed

proteins have functional roles in cell survival, DNA damage responses, and critical metabolic pathways that are important in tumor development. In the absence of a reliable animal model for the study of arsenic induced liver carcinogenesis, these proteomic data on the arsenic-induced regulation of proteins with important roles in tumor development may help elucidate the specific mechanisms underlying arsenic-induced liver carcinogenesis. To the best of our knowledge, this is the first study to analyze changes in the proteome in nonhuman primates exposed to arsenic.

5. References

[1] Smith AH, Goycolea M, Haque R, Biggs ML. Marked increase in bladder and lung cancer mortality in a region of Northern Chile due to arsenic in drinking water. Am J Epidemiol 1998; 147: 660–669.

[2] Hughes MF, Beck BD, Chen Y, Lewis AS, Thomas DJ. Arsenic exposure and toxicology: a historical perspective. Toxicol Sci 2011; 123: 305–332.

[3] Abernathy CO, Liu YP, Longfellow D, Aposhian HV, Beck B, Fowler B, Goyer R, Menzer R, Rossman T, Thompson C, Waalkes M. Arsenic: health effects, mechanisms of actions, and research issues. Environ Health Perspect 1999; 107: 593– 597.

[4] Tseng CH. Metabolism of inorganic arsenic and noncancerous health hazards associated with chronic exposure in humans. J Environ Biol 2007; 28: 349–357.

[5] Maull EA, Ahsan H, Edwards J, Longnecker MP, Navas-Acien A, Pi J, Silbergeld EK, Styblo M, Tseng CH, Thayer KA, Loomis D. Evaluation of the association between arsenic and diabetes: a National Toxicology Program workshop review. Environ Health Perspect 2012; 120: 1658–1670.

[6] Cooper KL, Liu KJ, Hudson LG. Contributions of reactive oxygen species and mitogen-activated protein kinase signaling in arsenite-stimulated hemeoxygenase- 1 production. Toxicol Appl Pharmacol 2007; 218: 119–127.

[7] Lynn S, Gurr JR, Lai HT, Jan KY. NADH oxidase activation is involved in arsenite-induced oxidative DNA damage in human vascular smooth muscle cells. Circ Res 2000; 86: 514–519.

[8] Wang Y, Xu Y, Wang H, Xue P, Li X, Li B, Zheng Q, Sun G. Arsenic induces mitochondria-dependent apoptosis by reactive oxygen species generation rather than glutathione depletion in Chang human hepatocytes. Arch Toxicol 2009; 83: 899–908.

[9] Li JJ, Tang Q, Li Y, Hu BR Ming ZY, Fu Q, Qian JQ, Xiang JZ. Role of oxidative stress in the apoptosis of hepatocellular carcinoma induced by combination of arsenic trioxide and ascorbic acid. Acta Pharmacol Sin 2006; 27: 1078–1084.

[10] Chang SI, Jin B, Youn P, Park C, Park JD, Ryu DY. Arsenic induced toxicity and the protective role of ascorbic acid in mouse testis. Toxicol Appl Pharmacol 2007; 218: 196–203.

[11] Muthumani M, Prabu SM. Silibinin potentially protects arsenic-induced oxidative hepatic dysfunction in rats. Toxicol Mech Methods 2012; 22: 277–88.

[12] Pari L, Mohamed Jalaludeen A. Protective role of sinapic acid against arsenic: induced toxicity in rats. Chem Biol Interact 2011; 194: 40–7.

[13] Liu J, Hinkhouse MM, Sun W, Weydert CJ, Ritchie JM, Oberley LW, Cullen JJ. Redox regulation of pancreatic cancer cell growth: role of glutathione peroxidase in the suppression of the malignant phenotype. Hum Gene Ther 2004; 15: 239–250.

[14] Lubos E, Loscalzo J, Handy DE. Glutathione peroxidase-1 in health and disease: from molecular mechanisms to

therapeutic opportunities. Antioxid Redox Signal 2011; 15: 1957–1997.

[15] Melchionna R, Chen XB, Blasina A, McGowan CH. Threonine 68 is required for radiation-induced phosphorylation and activation of Cds1. Nat Cell Biol 2000; 2: 762–765.

[16] Sato K, Ohta T, Venkitaraman AR. A mitotic role for the DNA damage-responsive CHK2 kinase. Nat Cell Biol 2010: 12; 424–425.

[17] Bonner WM, Redon CE, Dickey JS, Nakamura AJ, Sedelnikova OA, Solier S, Pommier Y. GammaH2AX and cancer. Nat Rev Cancer 2008; 8: 957–967.

[18] Prelich G, Tan CK, Kostura M, Mathews MB, So AG, Downey KM, Stillman B. Functional identity of proliferating cell nuclear antigen and a DNA polymerase-delta auxiliary protein. Nature 1987; 326: 517–520.

[19] Ulrich HD, Takahashi T. Readers of PCNA modifications. Chromosoma 2013; 122: 259–274.

[20] Watanabe K, Tateishi S, Kawasuji M, Tsurimoto T, Inoue H, Yamaizumi M. Rad18 guides poleta to replication stalling

sites through physical interaction and PCNA monoubiquitination. EMBO J 2004; 23: 3886–3896.

[21] Sakaguchi K, Herrera JE, Saito S, Miki T, Bustin M, Vassilev A, Anderson CW, Appella E. DNA damage activates p53 through a phosphorylationacetylation cascade. Genes Dev 1998; 12: 2831–2841.

[22] Jiang XH, Wong BC, Yuen ST, Jiang SH, Cho CH, Lai KC, Lin MC, Kung HF, Lam SK. Arsenic trioxide induces apoptosis in human gastric cancer cells through up-regulation of p53 and activation of caspase- 3. Int J Cancer 2001; 91: 173–179.

[23] Salazar AM, Ostrosky-Wegman P, Menéndez D, Miranda E, García-Carrancá A, Rojas E. Induction of p53 protein expression by sodium arsenite. Mutat Res 1997; 381: 259–265.

[24] Mitchell RD, Ayala-Fierro F, Carter DE. Systemic indicators of inorganic arsenic toxicity in four animal species. J Toxicol Environ Health A 2000; 59: 119–134.

[25] Pal S, Chatterjee AK. Prospective protective role of melatonin against arsenic-induced metabolic toxicity in Wistar rats. Toxicology 2005; 208: 25–33.

[26] Paul DS, Walton FS, Saunders RJ, Stýblo M. Characterization of the impaired glucose homeostasis produced in C57BL/6 mice by chronic exposure to arsenic and high-fat diet. Environ. Health Perspect 2011; 119: 1104-1109.

[27] Szinicz L, Forth W. Effect of As2O3 on gluconeogenesis. Arch Toxicol 1988; 61: 444-449.

[28] Dang Q, Kasibhatla SR, Reddy KR, Jiang T, Reddy MR, Potter SC, Fujitaki JM, van Poelje PD, Huang J, Lipscomb WN, Erion MD. Discovery of potent and specific fructose-1, 6-bisphosphatase inhibitors and a series of orally-bioavailable phosphoramidase-sensitive prodrugs for the treatment of type 2 diabetes. J Am Chem Soc 2007; 129: 15491-15502.

[29] Holyoak T, Sullivan SM, Nowak T. Structural insights into the mechanism of PEPCK catalysis. Biochemistry 2006; 45, 8254-8263.

[30] Cho YM, Bae SH, Choi BK, Cho SY, Song CW, Yoo JK, Paik YK. Differential expression of the liver proteome in senescence accelerated mice. Proteomics 2003; 3: 1883-1894.

[31] Shevchenko A, Wilm M, Vorm O, Mann M. Mass spectrometric sequencing of proteins silver-stained

polyacrylamide gels. Anal Chem 1996; 68: 850–858.

[32] Choi BK, Cho YM, Bae SH, Zoubaulis CC, Paik YK. Single-step perfusion chromatography with a throughput potential for enhanced peptide detection by matrix-assisted laser desorption/ionization-mass spectrometry. Proteomics 2003; 3: 1955–1961.

[33] Kim S, Lee SH, Kang S, Lee L, Park JD, Ryu DY. Involvement of c-Met- and phosphatidylinositol 3-kinase dependent pathways in arsenite-induced downregulation of catalase in hepatoma cells. Biol Pharm Bull 2011; 34: 1748–1752.

[34] Kannouche PL, Wing J, Lehmann AR. Interaction of human DNA polymerase eta with monoubiquitinated PCNA: a possiblemechanism for the polymerase switch in response to DNA damage. Mol Cell 2004; 14: 491–500.

[35] ATSDR, Toxicological Profile for Arsenic, Agency for Toxic Substances and Disease Registry, Public Health Service, US Department of Health and Human Services, Atlanta, GA 2007.

[36] Heywood R, Sortwell RJ. Arsenic intoxication in the

rhesus monkey. Toxicol Lett 1979; 3: 137–144.

[37] Vahter M, Marafante E, Lindgren A, Dencker L. Tissue distribution and subcellular binding of arsenic in marmoset monkeys after injection of 74As−arsenite. Arch Toxicol 1982; 51: 65–77.

[38] Thorgeirsson UP, Dalgard DW, Reeves J, Adamson RH. Tumor incidence in a chemical carcinogenesis study of nonhuman primates. Regul Toxicol Pharmacol 1994; 19: 130–151.

[39] Kaul SC, Aida S, Yaguchi T, Kaur K, Wadhwa R. Activation of wild type p53 function by its mortalin−binding, cytoplasmically localizing carboxyl terminus peptides. J Biol Chem 2005; 280: 39373–39379.

[40] Ma Z, Izumi H, Kanai M, Kabuyama Y, Ahn NG, Fukasawa K. Mortalin controls centrosome duplication via modulating centrosomal localization of p53. Oncogene 2006; 25: 5377–5390.

[41] Yi X, Luk JM, Lee NP, Peng J, Leng X, Guan XY, Lau GK, Beretta L, Fan ST. Association of mortalin (HSPA9) with liver cancer metastasis and prediction for early tumor recurrence.

Mol Cell Proteomics 2008; 7: 315–325.

[42] Li Y, Ling M, Xu Y, Wang S, Li Z, Zhou J, Wang X, Liu Q. The repressive effect of NF-kappaB on p53 by mot-2 is involved in human keratinocyte transformation induced by low levels of arsenite. Toxicol Sci 2010; 116: 174–182.

[43] Bégué E, Jean-Louis F, Bagot M, Jauliac S, Cayuela JM, Laroche L, Parquet N, Bachelez H, Bensussan A, Courtois G, Michel L. Inducible expression and pathophysiologic functions of T plastin in cutaneous T-cell lymphoma. Blood 2012; 120: 143–154.

[44] Sasaki Y, Itoh F, Kobayashi T, Kikuchi T, Suzuki H, Toyota M, Imai K. Increased expression of T-fimbrin gene after DNA damage in CHO cells and inactivation of T-fimbrin by CpG methylation in human colorectal cancer cells. Int J Cancer 2002; 97: 211–216.

[45] Ikeda H, Sasaki Y, Kobayashi T, Suzuki H, Mita H, Toyota M, Itoh F, Shinomura Y, Tokino T, Imai K. The role of T-fimbrin in the response to DNA damage: silencing of T-fimbrin by small interfering RNA sensitizes human liver cancer cells to DNA-damaging agents. Int J Oncol 2005; 27: 933–940.

[46] Hisano T, Ono M, Nakayama M, Naito S, Kuwano M, Wada M. Increased expression of T-plastin gene in cisplatin-resistant human cancer cells: identification by mRNA differential display. FEBS Lett 1996; 397: 101–107.

[47] Higuchi Y, Kita K, Nakanishi H, Wang XL, Sugaya S, Tanzawa H, Yamamori H, Sugita K, Yamaura A, Suzuki N. Search for genes involved in UV-resistance in human cells by mRNA differential display: increased transcriptional expression of nucleophosmin and T-plastin genes in association with the resistance. Biochem Biophys Res Commun 1998; 248: 597–602.

[48] Delhase M, Kim SY, Lee H, Naiki-Ito A, Chen Y, Ahn ER, Murata K, Kim SJ, Lautsch N, Kobayashi KS, Shirai T, Karin M, Nakanishi M. TANK binding kinase 1 (TBK1) controls cell survival through PAI-2/serpinB2 and transglutaminase 2. Proc Natl Acad Sci USA 2012; 109: E177–E186.

[49] Bonnard M, Mirtsos C, Suzuki S, Graham K, Huang J, Ng M, Itié A, Wakeham A, Shahinian A, Henzel WJ, Elia AJ, Shillinglaw W, Mak TW, Cao Z, Yeh WC. Deficiency of T2K leads to apoptotic liver degeneration and impaired NF-kappaB-dependent gene transcription. EMBO J 2000; 19: 4976–4985.

[50] Stipanuk MH. Sulfur amino acid metabolism: pathways for

production and removal of homocysteine and cysteine. Annu Rev Nutr 2004; 24: 539–577.

[51] Porter KE, Basu A, Hubbard AE, Bates MN, Kalman D, Rey O, Smith A, Smith MT, Steinmaus C, Skibola CF. Association of genetic variation in cystathionine-beta-synthase and arsenic metabolism. Environ Res 2010; 110: 580–587.

[52] Wu MM, Chiou HY, Hsueh YM, Hong CT, Su CL, Chang SF, Huang WL, Wang HT, Wang YH, Hsieh YC, Chen CJ. Effect of plasma homocysteine level and urinary monomethylarsonic acid on the risk of arsenic-associated carotid atherosclerosis. Toxicol Appl Pharmacol 2006; 216: 168–175.

[53] Kim J, Hong SJ, Park JH, Park SY, Kim SW, Cho EY, Do IG, Joh JW, Kim DS. Expression of cystathionine beta-synthase is downregulated in hepatocellular carcinoma and associated with poor prognosis. Oncol Rep 2009; 21: 1449–1454.

[54] Huang C, Ding G, Gu C, Zhou J, Kuang M, Ji Y, He Y, Kondo T, Fan J. Decreased selenium-binding protein 1 enhances glutathione peroxidase 1 activity and downregulates HIF-1α to promote hepatocellular carcinoma invasiveness. Clin Cancer Res 2012; 18: 3042–3053.

[55] Corona G, De Lorenzo E, Elia C, Simula MP, Avellini C, Baccarani U, Lupo F, Tiribelli C, Colombatti A, Toffoli G. Differential proteomic analysis of hepatocellular carcinoma. Int J Oncol 2010; 36: 93–99.

[56] Gerke V, Creutz CE, Moss SE. Annexins: linking Ca2+ signalling to membrane dynamics. Nat Rev Mol Cell Biol 2005; 6: 449–461.

[57] Vilá de Muga S, Timpson P, Cubells L, Evans R, Hayes TE, Rentero C, Hegemann A, Reverter M, Leschner J, Pol A, Tebar F, Daly RJ, Enrich C, Grewal T. Annexin A6 inhibits Ras signalling in breast cancer cells. Oncogene 2009; 28: 363–377.

[58] Grewal T, Evans R, Rentero C, Tebar F, Cubells L, de Diego I, Kirchhoff MF, Hughes WE, Heeren J, Rye KA, Rinninger F, Daly RJ, Pol A, Enrich C. Annexin A6 stimulates the membrane recruitment of p120GAP to modulate Ras and Raf-1 activity. Oncogene 2005; 24: 5809–5820.

[59] Smith DL, Evans CA, Pierce A, Gaskell SJ, Whetton AD. Changes in the proteome associated with the action of Bcr-Abl tyrosine kinase are not related to transcriptional regulation. Mol Cell Proteomics 2002; 1: 876–884.

[60] Díaz-Ramos A, Roig-Borrellas A, García-Melero A, López-Alemany R. α-Enolase, a multifunctional protein: its role on pathophysiological situations. J Biomed Biotechnol 2012; 2012: 156795.

[61] Luo Q, Jiang L, Chen G, Feng Y, Lv Q, Zhang C, Qu S, Zhu H, Zhou B, Xiao X. Constitutive heat shock protein 70 interacts with α-enolase and protects cardiomyocytes against oxidative stress. Free Radic Res 2011; 45: 1355–1365.

[62] Lii CK, Lin AH, Lee SL, Chen HW, Wang TS. Oxidative modifications of proteins by sodium arsenite in human umbilical vein endothelial cells. Environ Toxicol 2011; 26: 459–471.

[63] Pearce MM, Wang Y, Kelley GG, Wojcikiewicz RJ. SPFH2 mediates the endoplasmic reticulum-associated degradation of inositol 1,4,5-trisphosphate receptors and other substrates in mammalian cells. J Biol Chem 2007; 282: 20104–20115.

[64] Burke AJ, Sullivan FJ, Giles FJ, Glynn SA. The yin and yang of nitric oxide in cancer progression. Carcinogenesis 2013; 34: 503–512.

[65] Chrzanowska A, Gajewska B, Barańczyk-Kuźma A. Changes in arginase isoenzymes pattern in human hepatocellular carcinoma. Biochem Biophys Res Commun 2008; 377: 337–340.

[66] Kletzien RF, Harris PK, Foellmi LA. Glucose-6-phosphate dehydrogenase: a “housekeeping” enzyme subject to tissue-specific regulation by hormones, nutrients, and oxidant stress. FASEB J 1994; 8: 174–181.

[67] Lee JW, Choi AH, Ham M, Kim JW, Choe SS, Park J, Lee GY, Yoon KH, Kim JB. G6PD upregulation promotes pancreatic beta-cell dysfunction. Endocrinology 2011; 152: 793–803.

[68] Ham M, Lee JW, Choi AH, Jang H, Choi G, Park J, Kozuka C, Sears DD, Masuzaki H, Kim JB. Macrophage glucose-6-phosphate dehydrogenase stimulates proinflammatory responses with oxidative stress. Mol Cell Biol 2013; 33: 2425–2435.

[69] de Haan JB, Bladier C, Griffiths P, Kelner M, O'Shea RD, Cheung NS, Bronson RT, Silvestro MJ, Wild S, Zheng SS, Beart PM, Hertzog PJ, Kola I. Mice with a homozygous nullmutation for themost abundant glutathione peroxidase, Gpx1, show increased susceptibility to the oxidative stress-inducing agents

paraquat and hydrogen peroxide. J Biol Chem 1998; 273: 22528–22536.

[70] Kitchin KT. Recent advances in arsenic carcinogenesis: modes of action, animal model systems, and methylated arsenic metabolites. Toxicol Appl Pharmacol 2001; 172: 249–261.

[71] Druwe IL, Vaillancourt RR. Influence of arsenate and arsenite on signal transduction pathways: an update. Arch Toxicol 2010; 84: 585–596.

[72] Kaltreider RC, Davis AM, Lariviere JP, Hamilton JW. Arsenic alters the function of the glucocorticoid receptor as a transcription factor. Environ. Health Perspect 2001; 109: 245–251.

[73] Chanda D, Kim SJ, Lee IK, Shong M, Choi HS. Sodium arsenite induces orphan nuclear receptor SHP gene expression via AMP−activated protein kinase to inhibit gluconeogenic enzyme gene expression. Am J Physiol Endocrinol Metab 2008; 295: E368–E379.

[74] Sutherland C, Tebbey PW, Granner DK. Oxidative and chemical stress mimic insulin by selectively inhibiting the expression of phosphoenolpyruvate carboxykinase in hepatoma

cells. Diabetes 1997; 46: 17–22.

[75] Radziuk J, Pye S. Hepatic glucose uptake, gluconeogenesis and the regulation of glycogen synthesis. Diabetes Metab Res Rev 2001; 17: 250–272.

[76] Barthel A, Schmoll D. Novel concepts in insulin regulation of hepatic gluconeogenesis. Am J Physiol Endocrinol Metab 2003; 285: E685–E692.

[77] Cárcamo JG, Yañez AJ, Ludwig HC, León O, Pinto RO, Reyes AM, Slebe JC. The C1−C2 interface residue lysine 50 of pig kidney fructose−1, 6−bisphosphatase has a crucial role in the cooperative signal transmission of the AMP inhibition. Eur J Biochem 2000; 267: 2242–2251.

[78] Yañez AJ, Ludwig HC, Bertinat R, Spichiger C, Gatica R, Berlien G, Leon O, Brito M, Concha II, Slebe JC. Different involvement for aldolase isoenzymes in kidney glucose metabolism: aldolase B but not aldolase A colocalizes and forms a complex with FBPase. J Cell Physiol 2005; 202: 743–753.

[79] Wang B, Hsu SH, Frankel W, Ghoshal K, Jacob ST. Stat3−mediated activation of microRNA−23a suppresses gluconeogenesis in hepatocellular carcinoma by down−

regulating glucose-6-phosphatase and peroxisome proliferator-activated receptor gamma, coactivator 1 alpha. Hepatology 2012; 56: 186-197.

[80] Cao G, Liang Y, Broderick CL, Oldham BA, Beyer TP, Schmidt RJ, Zhang Y, Stayrook KR, Suen C, Otto KA, Miller AR, Dai J, Foxworthy P, Gao H, Ryan TP, Jiang XC, Burris TP, Eacho PI, Etgen GJ. Antidiabetic action of a liver x receptor agonist mediated by inhibition of hepatic gluconeogenesis. J Biol Chem 2003; 278: 1131-1136.

[81] Stulnig TM, Steffensen KR, Gao H, Reimers M, Dahlman-Wright K, Schuster GU, Gustafsson JA. Novel roles of liver X receptors exposed by gene expression profiling in liver and adipose tissue. Mol Pharmacol 2002; 62: 1299-1305.

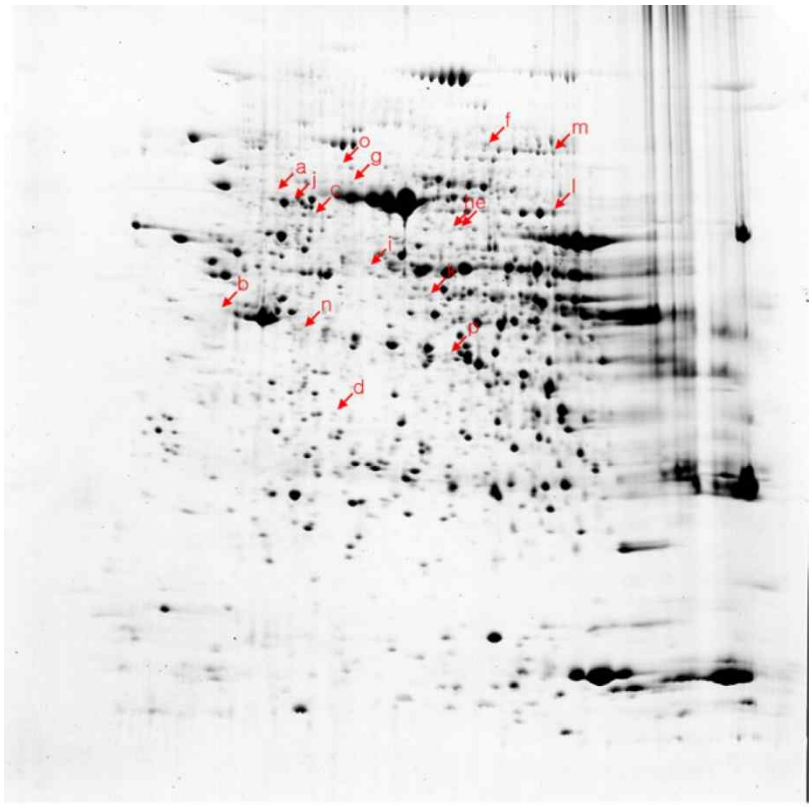

Figure 1. 2D-PAGE analysis of hepatic proteins from SA-treated and control monkeys. A representative image from a control liver tissue is shown. Comparative analysis of equivalent spots between SA-treated and control groups identified 16 spots (a to p) with differential expression of more than fivefold change and $p \leq 0.05$. (a) mortalin, (b) tubulin beta chain, (c) plastin-3, (d) leucine-rich repeat-containing protein 16B, (e) coatomer subunit delta, (f) serine/threonine-protein kinase TBK1, (g) peroxisomal bifunctional enzyme, (h) CBS, (i) SBP1, (j) annexin A6, (k) alphaenolase, (l) PEPCK-M, (m) probable guanine nucleotide exchange factor MCF2L2, (n) erlin-2, (o) keratin, type II cytoskeletal 1, and (p) arginase-1.

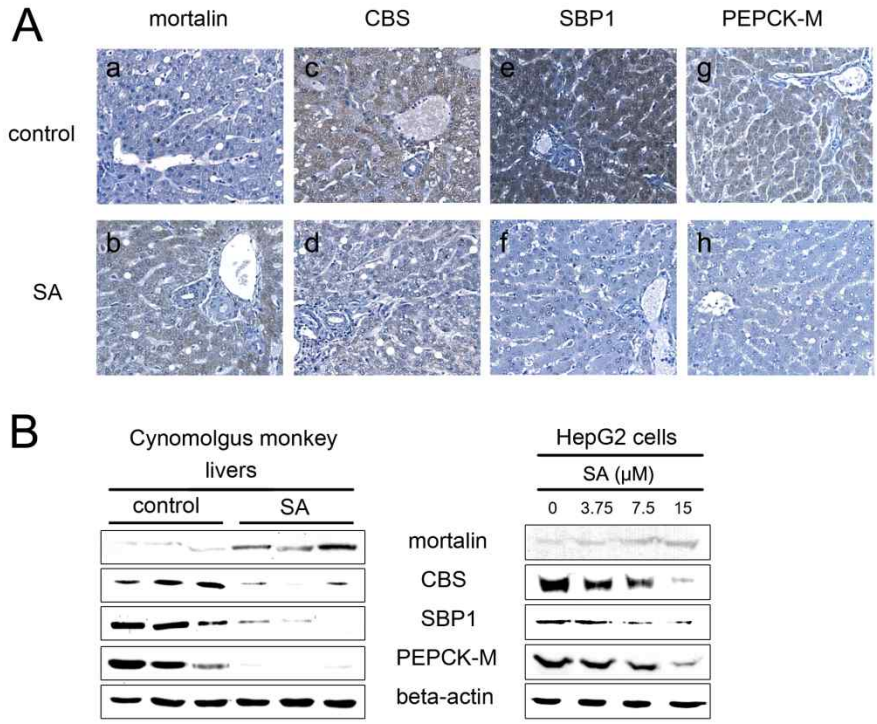

Figure 2. Expression levels of mortalin, CBS, SBP1, and PEPCK-M in SA-treated monkey liver tissues and HepG2 cells. Data are representative of three to four independent experiments. (A) IHC analysis of mortalin (a and b), CBS (c and d), SBP1 (e and f), and PEPCK-M (g and h) proteins in control-treated (a, c, e, and g) and SAtreated monkey livers (b, d, f, and h). Magnification, ×400. (B) Western blot analysis of mortalin, CBS, SBP1, and PEPCKM in SA-treated monkey liver tissues and HepG2 cells. Beta-actin was used as an internal control.

Figure 3. Western blot analysis of the oxidative stress-related proteins, G6PD, GPx-1, catalase, and GR, in SA-treated monkey liver tissues and HepG2 cells. Data are representative of three to four independent experiments. Beta-actinwas used as an internal control, as shown in Figure 2.

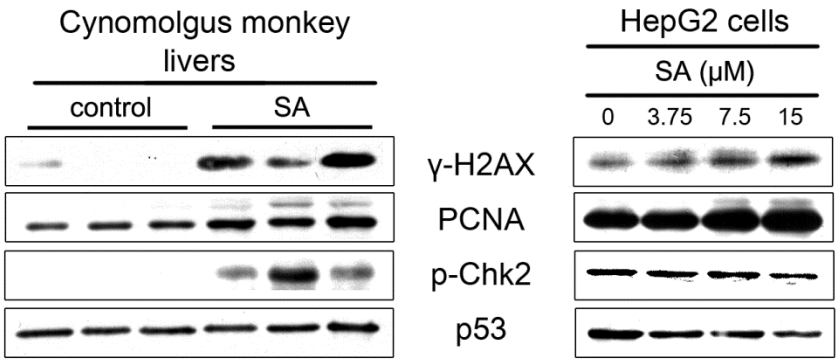

Figure 4. Western blot analysis of the DNA damage-related proteins, γ-H2AX, PCNA, p-Chk2, and p53, in SA-treated monkey liver tissues and HepG2 cells. Data are representative of three to four independent experiments. Beta-actinwas used as an internal control, shown in Figure 2.

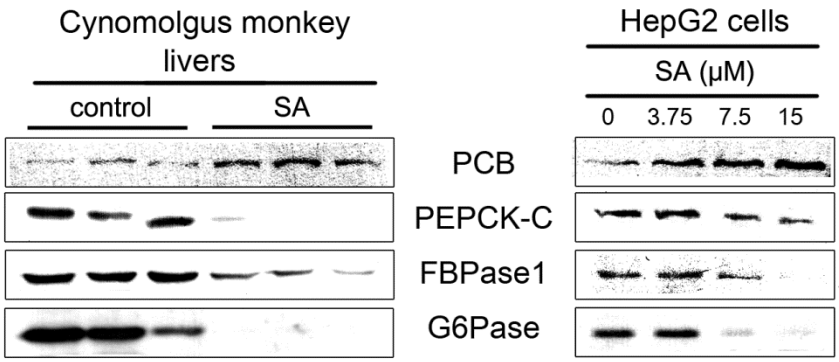

Figure 5. Western blot analysis of the gluconeogenesis-related proteins, PCB, PEPCK-C, FBPase1, and G6Pase, in SA-treated monkey liver tissues and HepG2 cells. Data are representative of three to four independent experiments. Beta-actin was used as an internal control, shown in Figure 2.

Table 1. Proteins showing increased expression in the livers of cynomolgus monkeys treated with SA. The fold change reflects the quotient of two corresponding spot volumes (SA−treated/control)

Fold change	Accession #	Protein	Sequence coverage (%)	Mascot score	Biological process	Identification methods
8.8	gi|12653415	Stress-70 protein, mitochondrial; mortalin	25	67	Cellular protein metabolic process Negative regulation of apoptotic process	MS, WB, IHC
7.8	gi|57209813	Tubulin beta chain	34	113	Microtubule-based movement	MS

The sequence coverage refers to the observed sequence coverage of the assigned protein. Protein identifications were considered as reliable when the Mascot score was higher than 66 ($p < 0.05$). Mascot score was calculated as $-10 \times \log(p)$, where p is the probability that the observed match is considered a random event.

Table 2. Proteins showing decreased expression in the livers of cynomolgus monkeys treated with SA. The fold change reflects the quotient of two corresponding spot volumes (control/SA-treated)

Fold change	Accession #	Protein	Sequence coverage (%)	MASCOT score	Biological process	Identification methods
12.6	gi|190028	Plastin-3	38	117		MS
11.6	gi|21739700	Leucine-rich repeat-containing protein 16B	36	71		MS
10.3	gi|11863154	Coatomer subunit delta	38	130	Intracellular protein transport	MS
9.1	gi|7019547	Serine/threonine-protein kinase TBK1	24	69	Antiviral defense Innate immunity	MS
8.5	gi|68989263	Peroxisomal bifunctional enzyme	27	77	Fatty acid beta-oxidation Internal protein amino acid acetylation	MS, MS/MS
8.3	gi|3850687	Cystathionine beta-synthase; CBS	25	80	Cysteine biosynthetic process via cystathionine Superoxide metabolic process	MS, WB, IHC
7.8	gi|16306550	Selenium-binding protein 1; SBP1	50	165	Protein transport	MS, WB, IHC

7.7	gi|71773329	Annexin A6	37	136	Calcium ion transport	MS
7.5	gi|4503571	Alpha-enolase	32	69	Glycolysis Plasminogen activation Transcription regulation	MS, MS/MS
7.2	gi|12655193	Phosphoenolpyruvate carboxykinase [GTP], mitochondrial; PEPCK-M	33	169	Gluconeogenesis	MS, WB, IHC
6.4	gi|27752365	Probable guanine nucleotide exchange factor MCF2L2	22	70	Regulation of Rho protein signal transduction	MS
5.9	gi|6005721	Erlin-2	44	82	ER-associated protein catabolic process Cell death	MS
5.2	gi|11935049	Keratin, type II cytoskeletal 1	30	220	Epidermis development Response to oxidative stress	MS
5.0	gi|10947139	Arginase-1	32	76	Urea cycle Cellular response to hydrogen peroxide	MS, MS/MS

The sequence coverage refers to the observed sequence coverage of the assigned protein. Protein identifications were considered as reliable when the Mascot score was higher than 66 ($p < 0.05$). Mascot score was calculated as $-10 \times \log(p)$, where p is the probability that the observed match is considered a random event.

CHAPTER Ⅱ

INVOLVEMENT OF C-MET- AND PHOSPHATIDYLINOSITOL 3-KINASE DEPENDENT PATHWAYS IN ARSENITE-INDUCED DOWNREGULATION OF CATALASE IN HEPATOMA CELLS

1. Introduction

Cellular defense systems, including a variety of antioxidant molecules and enzymes such as superoxide dismutase, glutathione peroxidase and catalase, ensure that reactive oxygen species (ROS) are maintained at relatively low levels in normal conditions [1]. Arsenic and its compounds are well documented environmental toxicants [2] that induce oxidative damage by increasing the production of ROS. Oxidative damage has been suggested to play a key role in arsenicinduced toxicity [3–7].

Catalase protects cells from ROS–induced damage by catalyzing the breakdown of hydrogen peroxide (H2O2) into oxygen and water. Arsenic has been demonstrated to decrease catalase expression both in animal tissues and cultured cells. Catalase activity is significantly decreased in the liver of rats treated with arsenite [8–10]. Arsenite treatment *in vitro* decreases catalase activity in human fibroblasts [4]. In a human keratinocyte cell line, it was also shown to decrease levels of catalase mRNA and protein.11)

Phosphatidylinositol 3–kinases (PI3Ks) are key components for the activation of Akt signaling. In the PI3K/Akt pathway, formation of 3–phosphoinositides by PI3K enables the activation of Akt by phosphoinositide–dependent protein kinases 1 and 2, which phosphorylate Akt at threonine

residue 308 (Thr308) and serine residue 473 (Ser473), respectively. PI3K/Akt is thought to play a pivotal role in regulating cell proliferation, survival, metabolism and cancer progression. The PI3K/Akt pathway is downstream of c-Met receptor tyrosine kinase, a receptor for hepatocyte growth factor [12-14]. In c-Met-deficient mouse hepatocytes, the level of catalase protein is constitutively high [15], suggesting that a c-Met-dependent pathway is involved in catalase expression. Rat liver epithelial cells transformed by chronic exposure to arsenite show upregulated c-Met expression [16].

Some studies indicate that arsenite induces the activation of PI3K/Akt. In human keratinocytes, for example, it induces the phosphorylation of Akt at both Ser473 and Thr308, which is inhibited by treatment with PI3K inhibitors such as Wortmannin and LY294002 (LY) [17]. Arsenite-induced activation of both PI3K and Akt and the attenuation of arseniteinduced activation of Akt by PI3K inhibitors have also been demonstrated in human prostate carcinoma cells [18] and mouse epidermal cells [19].

PI3K/Akt plays an important role in regulating catalase expression. Venkatesan et al. examined the role of PI3K/Akt in H2O2-induced downregulation of catalase in mesangial cells [20]. They found that LY significantly attenuates the inhibitory effect of H2O2 on the level of catalase protein and

that the expression of the tumor suppressor protein phosphatase and tensin homolog (PTEN), a modulator of PI3K pathway [21,22], increases catalase protein levels. It is the expression of dominant negative Akt that significantly activates the catalase gene promoter and prevents the inhibitory effect of H2O2 on the catalase protein level.

Previous studies have demonstrated arsenite-induced activation of PI3K and c-Met- and PI3K-dependent inhibition of catalase expression. The aim of this study was to examine the involvement of c-Met- and PI3K-dependent pathways in arsenite- induced inhibition of catalase expression. Catalase mRNA and protein expression have been analyzed in human hepatoma cells treated with sodium arsenite and an inhibitor of either c-Met or PI3K.

2. Material and methods

2.1. Chemicals

All chemicals used were of reagent grade or higher and were obtained from Sigma-Aldrich (St. Louis, MO, U.S.A.), unless otherwise specified.

2.2. Cell Treatment

Human hepatoma cell line HepG2 was grown in RPMI 1640 medium with 2 mg/ml sodium bicarbonate, 10% (v/v) fetal bovine serum, 100 units/ml penicillin and 100m g/ml streptomycin. The cells were maintained at 37 ℃ in a 5% CO2 incubator. Twenty-four hours after the cells were plated, the culture medium was removed and replaced with medium containing various concentrations of sodium arsenite. Solutions of c-Met inhibitor PHA665752 ((PHA), Santa Cruz Biotechnology, Santa Cruz, CA, U.S.A.) and PI3K inhibitor LY (BioVision, Mountain View, CA, U.S.A.) dissolved in dimethylsulfoxide (DMSO) were added to the culture plates. The final concentration of DMSO in both control and test cultures did not exceed 0.05%. For the c-Met and PI3K inhibition studies, HepG2 cells were treated with PHA for 4 h followed by sodium arsenite for 24 h [23,24], and co-treated with LY and sodium arsenite for 24 h [25,26], respectively.

2.3. Cell Viability

3-(4,5-Dimethylthiazol-2-yl)-2,5-diphenyltetrazoliu m bromide (MTT) reduction was used to assess cell viability [27]. Briefly, 10× MTT stock solution (5 mg/ml in phosphate

buffered saline, pH 7.4) was added to each culture well, and the plates were incubated at 37 ℃ for 4 h. The MTT solution was then aspirated and 0.2 ml of acidified isopropanol (0.04 N HCl in isopropanol) was added to each well to dissolve the formazan. After 2—3 min at room temperature, the plates were analyzed using a microplate reader (Molecular Devices, Sunnyvale, CA, U.S.A.) at a wavelength of 560 nm.

2.4. Real-Time Reverse Transcription-Polymerase Chain Reaction (RT-PCR)

Total RNA was extracted from HepG2 cells using Trizol reagent (Invitrogen, Carlsbad, CA, U.S.A.) according to the manufacturer's instructions. The amount of RNA in each sample was quantified using a Nanodrop ND-1000 spectrophotometer (NanoDrop Technologies, Wilmington, DE, U.S.A.) and 1m g of total RNA was reverse transcribed using reverse transcriptase and random hexamers (Promega, Madison, WI, U.S.A.). Real-time RT-PCR was performed with cDNAs and gene-specific primers (Table 1) using ABI SYBR Green PCR master mix (Applied Biosystems, Foster City, CA, U.S.A.) in an ABI Prism 7000 thermocycler (Applied Biosystems). Samples were first denatured for 10 min at 95 ℃ and then subjected to forty cycles of

amplification and quantification (15 s at 95 ℃, 1 min at 60 ℃), followed by a melting curve program (60—99 ℃ with a heating rate of 0.1 ℃/s and continuous fluorescence measurement). Western Blot Total proteins were extracted from HepG2 cells with a Pro-Prep protein extraction kit (Intron, Kyungkido, Korea) and protein concentration was determined with a Pro-Measure kit (Intron) according to the manufacturer's instructions. Samples containing 10 μg of protein were denatured by boiling for 10 min in 5 × sodium dodecyl sulfate (SDS) gel loading buffer (5% SDS; 0.225 M Tris, pH 6.8; 50% glycerol; 0.05% bromophenol blue; 0.25 M dithiothreitol), separated by SDS-polyacrylamide gel electrophoresis, and then transferred to nitrocellulose membranes. The membranes were incubated with mouse anti-catalase antibody (ab16731, Abcam, Cambridge, MA, U.S.A.), rabbit anti-Akt antibody (#9272, Cell Signaling Technology, Beverly, MA, U.S.A.), rabbit anti-phospho-Akt (Ser473) antibody (#9271, Cell Signaling Technology), rabbit anti-phospho- Akt (Thr308) antibody (#4056, Cell Signaling Technology) and mouse anti-β-actin antibody (A5441), followed by incubation with horse-radish peroxidase (HRP)-conjugated sheep anti-mouse immunoglobulin G (IgG) (NA931, Amersham Biosciences, Arlington Heights, IL, U.S.A.) or HRP conjugated donkey anti-rabbit IgG (NA934, Amersham Biosciences) as secondary antibody. Blots were

developed using a chemiluminescence detection reagent kit. The Western blot procedure provides a qualitative, not quantitative, comparison between samples; therefore, no statistical analysis was performed.

2.5. Statistical Analysis

All data are expressed as mean_ standard deviation (S.D.), and the non-parametric Mann- Whitney U test was used to compare selected pairs of groups. An IC50 value was determined by probit analysis. All statistical analyses were performed using SPSS 18 software (SPSS, Chicago, IL, U.S.A.). A p-value of less than 0.05 was considered significant.

3. Results

3.1. Cytotoxicity

To assess the cytotoxic effects of arsenite on HepG2 cells, the MTT assay was used as a measure of cell viability. Cells were incubated for 24 h with different doses of arsenite ranging from 2.5 μM up to 80 μM (Figure 1). Cell viability significantly decreased in a dose-dependent manner after a

24 h treatment with arsenite doses of 20 μM or higher, and the IC50 (the dose required for 50% reduction in cell viability) of arsenite was calculated to be 27.5±2.40 μM. In all subsequent experiments, the highest concentration of arsenite used to treat cells was 15 μM, approximately half the IC50.

3.2. Inhibition of Catalase Expression

Next, the expression of catalase mRNA and protein in arsenite-treated HepG2 cells was investigated. Arsenite treatment decreased catalase mRNA levels in a dose-dependent manner (Figure 2A). Catalase mRNA expression was decreased 1.7-, 1.8- and 3.4-fold compared to untreated controls (UC) after treatment with arsenite at 3.75, 7.5 and 15 μM, respectively. Compared with UC, arsenite also markedly decreased the level of catalase protein in the cells in a dose-dependent manner (Figure 2B).

3.3. Expression of MT1b and HO-1 mRNA

To study the effect of arsenite on the expression of oxidative stress-responsive gene products [28], levels of metallothionein 1b (MT1b) and heme oxygenase-1 (HO-1) mRNA in arsenite-treated cells were analyzed. Like catalase,

both MT1b and HO-1 play an important role in scavenging cellular ROS. Consistent with previous studies [29,30], the mRNA levels of MT1b and HO-1 were increased significantly compared to UC after 24 h treatment with arsenite doses of 3.75 μM or higher (Figure 3). Thus, whereas catalase expression is inhibited in arsenite-treated cells (Figure 2), expression of the functionally- related genes, MT1b and HO-1, is up-regulated.

3.4. Activation of Akt

Previous studies have demonstrated arsenite-induced activation of Akt in a variety of cells [17-19]. To determine whether Akt is activated in HepG2 cells after treatment with arsenite, phosphorylation of Akt at Ser473 and Thr308 was examined. Arsenite markedly induced Akt phosphorylation of both residues in a dose-dependent manner, while the level of total Akt protein remained unaffected (Figure 4).

3.5. Effect of a c-Met Inhibitor

Since c-Met deficiency has been shown to increase the level of catalase protein in mouse hepatocytes [15], the effect of a c-Met inhibitor PHA on catalase regulation in

arsenite-treated cells was investigated (Figure 5). The level of Akt protein in the cells was unaffected by treatment with PHA alone. PHA, however, blocked arsenite-induced Akt phosphorylation at Ser473 and Thr308 and attenuated the inhibitory effect of arsenite on catalase protein level in a dose-dependent manner (Figure 5A). These findings indicate that a c-Met pathway is responsible for the reduced expression of catalase protein in arsenite-treated cells. PHA treatment also increased the catalase protein level in cells that were not treated with arsenite.

To determine whether attenuation by PHA of arsenite induced catalase protein expression inhibition results from a change in mRNA levels, real-time RT-PCR was performed (Figure 5B). In contrast to the inhibitory effect of PHA on catalase protein levels (Figure 5A), it did not affect the level of catalase mRNA in arsenite-treated and -untreated cells. These findings indicate that c-Met is not involved in regulating catalase mRNA expression in HepG2 cells.

3.6. Effect of PI3K Inhibition

The PI3K inhibitor LY had a similar effect on catalase expression in HepG2 cells to PHA (Figure 6). LY treatment attenuated arsenite-induced Akt phosphorylation at Ser473 and Thr308 in a dose-dependent manner, while the Akt

protein level was not affected (Figure 6A). The catalase protein level increased after LY treatment in arsenite-treated cells, suggesting that inactivation of PI3K attenuates the arsenite-induced decrease in catalase protein levels. LY treatment also increased the level of catalase protein in the cells that were not treated with arsenite.

To determine whether the change in the level of catalase was a result of a change in the level of catalase mRNA, catalase real-time RT-PCR was carried out on cells treated with LY and arsenite (Figure 6B). In contrast to the inhibitory effect of LY on catalase protein levels, LY, like PHA, did not block arsenite-induced inhibition of catalase mRNA expression in the cells (Figure 5). These findings suggest that PI3K is not involved in arsenite-induced inhibition of catalase mRNA expression in HepG2 cells.

4. Discussion

The aim of this study was to investigate the involvement of c-Met- and PI3K-dependent-pathways in arsenite-induced inhibition of catalase expression. In agreement with other studies of cultured cells and animal tissues, arsenite-induced inhibition of catalase expression was demonstrated. Interestingly, a decrease in the gene expression of catalase, a major ROS-scavenging enzyme, occurred in cells where

oxidative stress-responsive gene products such as MT1b and HO-1 were highly up-regulated. Based upon the catalytic characteristics of catalase, reduced catalase activity in cells undergoing oxidative stress is likely to predispose those cells to H2O2-induced toxicity.

How catalase expression is regulated during oxidative stress is unclear. Catalase activity, protein and/or mRNA levels have been found to be increased [31-33], unchanged [34] or decreased [35-42] during oxidative stress. A ROS-mediated, biphasic model of catalase regulation has, however, been proposed in which catalase is stimulated by c-Abl/Arg-mediated phosphorylation at lower ROS levels [43], while in the event of uncontrollable ROS levels, catalase is degraded by ubiquitin-mediated proteasomal proteolysis, which thereby induces cell death. It has also been shown that treatment with ceramides, which induce oxidative damage, results in proteolytic cleavage of catalase by activated caspase-3 [44]. Since arsenitetreated cells are in a state of high oxidative stress, as indicated by the marked induction of MT1b and HO-1 expression, it is possible that catalase is subject to proteolytic degradation in these cells.

This study has provided the first evidence for the involvement of c-Met and PI3K pathways in the arsenite-induced inhibition of catalase expression. Inactivation of c-Met and PI3K led to increased levels of catalase protein in

both arsenite-treated and -untreated cells, with no effect on the level of catalase mRNA. These findings suggest that the primary effect of c-Met and PI3K inactivation on catalase levels in HepG2 cells occurs post-transcriptionally. Since c-Met and PI3K inhibitors both affected the arsenite-induced inhibition of catalase expression similarly, it is likely that a c-Met/PI3K/Akt pathway is involved in post-transcriptional regulation of catalase in arsenite-treated HepG2 cells.

Venkatesan et al. reported that ROS treatment inhibits the transcription of catalase in mesangial cells [20]. The arsenite induced decrease in catalase mRNA found in the present study could plausibly be the result of transcriptional inhibition. However, in the same report, dominant negative Akt was shown to increase catalase mRNA in mesangial cells; this is inconsistent with the observation presented here that Akt inactivation did not enhance the levels of catalase mRNA. The specific mechanisms underlying this apparent discrepancy remain to be elucidated.

In summary, the findings of the present study suggest that arsenite-induced inhibition of catalase expression is regulated at the mRNA and post-transcriptional levels in hepatoma cells, and that post-transcriptional regulation of catalase is mediated via c-Met- and PI3K-dependent mechanisms.

5. References

[1] Remacle J, Lambert D, Raes M, Pigeolet E, Michiels C, Toussaint O. Importance of various antioxidant enzymes for cell stability. Confrontation between theoretical and experimental data. Biochem J 1992; 286:41-46.

[2] Ishinishi N, Tsuchiya K, Vahter M, Fowler BA. "Arsenic: Handbook on the Toxicology of Metals," ed. by Friberg L, Nondberg GF, Vouk V. Elsevier, Amsterdam, 1986, pp. 43—83.

[3] Lynn S, Gurr JR, Lai HT, Jan KY. NADH oxidase activation is involved in arsenite-induced oxidative DNA damage in human vascular smooth muscle cells. Circ Res 2000; 86:514-519.

[4] Lee TC, Ho IC. Modulation of cellular antioxidant defense activities by sodium arsenite in human fibroblasts. Arch Toxicol 1995; 69:498-504.

[5] Lau AT, He QY, Chiu JF. A proteome analysis of the arsenite response in cultured lung cells: evidence for in vitro oxidative stress-induced apoptosis. Biochem J 2004; 382: 641-650.

[6] Li M, Cai JF, Chiu JF. Arsenic induces oxidative stress and activates stress gene expressions in cultured lung epithelial cells. J Cell Biochem 2002; 87:29-38.

[7] Chang SI, Jin B, Youn P, Park C, Park JD, Ryu DY. Arsenic-induced toxicity and the protective role of ascorbic acid in mouse testis. Toxicol Appl Pharmacol 2007; 218: 196-203.

[8] Bashir S, Sharma Y, Irshad M, Gupta SD, Dogra TD. Arsenic-induced cell death in liver and brain of experimental rats. Basic Clin Pharmacol Toxicol 2006; 98: 38-43.

[9] Bashir S, Sharma Y, Irshad M, Nag TC, Tiwari M, Kabra M, Dogra TD. Arsenic induced apoptosis in rat liver following repeated 60 days exposure. Toxicology 2006; 217: 63-70.

[10] Gupta R, Flora SJ. Protective value of Aloe vera against some toxic effects of arsenic in rats. Phytother Res 2005; 19:23-28.

[11] Sun X, Li B, Li X, Wang Y, Xu Y, Jin Y, Piao F, Sun G. Effects of sodium arsenite on catalase activity, gene and protein expression in HaCaT cells. Toxicol In Vitro 2006; 20: 1139-1144.

[12] Royal I, Park M. Hepatocyte growth factor-induced scatter of Madin-Darby canine kidney cells requires phosphatidylinositol 3-kinase. J Biol Chem 1995; 270: 27780-27787.

[13] Ponzetto C, Bardelli A, Maina F, Longati P, Panayotou G, Dhand R, Waterfield MD, Comoglio PM. A novel recognition motif for phosphatidylinositol 3-kinase binding mediates its association with the hepatocyte growth factor/scatter factor receptor. Mol Cell Biol 1993; 13:4600-4608.

[14] Whittaker S, Marais R, Zhu AX. The role of signaling pathways in the development and treatment of hepatocellular carcinoma. Oncogene. 2010; 29: 4989-5005.

[15] Gómez-Quiroz LE, Factor VM, Kaposi-Novak P, Coulouarn C, Conner EA, Thorgeirsson SS. Hepatocyte-specific c-Met deletion disrupts redox homeostasis and sensitizes to Fas-mediated apoptosis. J Biol Chem 2008; 283: 14581-14589.

[16] Liu J, Benbrahim-Tallaa L, Qian X, Yu L, Xie Y, Boos J, Qu W, Waalkes MP. Further studies on aberrant gene expression associated with arsenic-induced malignant transformation in rat liver TRL1215 cells. Toxicol Appl Pharmacol 2006; 216: 407-

415.

[17] Souza K, Maddock DA, Zhang Q, Chen J, Chiu C, Mehta S, Wan Y. Arsenite activation of P13K/AKT cell survival pathway is mediated by p38 in cultured human keratinocytes. Mol Med 2001; 7: 767-772.

[18] Gao N, Shen L, Zhang Z, Leonard SS, He H, Zhang XG, Shi X, Jiang BH. Arsenite induces HIF-1alpha and VEGF through PI3K, Akt and reactive oxygen species in DU145 human prostate carcinoma cells. Mol Cell Biochem 2004; 255: 33-45.

[20] Venkatesan B, Mahimainathan L, Das F, Ghosh-Choudhury N, Ghosh Choudhury G. Downregulation of catalase by reactive oxygen species via PI 3 kinase/Akt signaling in mesangial cells. J Cell Physiol 2007; 211: 457-467.

[21] Maehama T, Dixon JE. The tumor suppressor, PTEN/MMAC1, dephosphorylates the lipid second messenger, phosphatidylinositol 3,4,5-trisphosphate. J Biol Chem 1998; 273: 13375-13378.

[22] Lian Z, Di Cristofano A. Class reunion: PTEN joins the nuclear crew. Oncogene 2005; 24: 7394-7400.

[23] Christensen JG, Schreck R, Burrows J, Kuruganti P, Chan E, Le P, Chen J, Wang X, Ruslim L, Blake R, Lipson KE, Ramphal J, Do S, Cui JJ, Cherrington JM, Mendel DB. A selective small molecule inhibitor of c-Met kinase inhibits c-Met-dependent phenotypes in vitro and exhibits cytoreductive antitumor activity in vivo. Cancer Res 2003; 63: 7345-7355.

[24] Kongkham PN, Onvani S, Smith CA, Rutka JT. Inhibition of the MET Receptor Tyrosine Kinase as a Novel Therapeutic Strategy in Medulloblastoma. Transl Oncol 2010; 3: 336-343.

[25] Urbich C, Knau A, Fichtlscherer S, Walter DH, Brühl T, Potente M, Hofmann WK, de Vos S, Zeiher AM, Dimmeler S. FOXO-dependent expression of the proapoptotic protein Bim: pivotal role for apoptosis signaling in endothelial progenitor cells. FASEB J 2005; 19:974-976.

[26] Laplante P, Raymond MA, Gagnon G, Vigneault N, Sasseville AM, Langelier Y, Bernard M, Raymond Y, Hébert MJ. Novel fibrogenic pathways are activated in response to endothelial apoptosis: implications in the pathophysiology of systemic sclerosis. J Immunol 2005; 174: 5740-5749.

[27] Mosmann T. Rapid colorimetric assay for cellular growth and survival: application to proliferation and cytotoxicity assays.

J Immunol Methods 1983; 65: 55-63.

[28] Fu K, Sarras MP Jr, De Lisle RC, Andrews GK. Expression of oxidative stress-responsive genes and cytokine genes during caerulein-induced acute pancreatitis. Am J Physiol 1997; 273: G696-705.

[29] Elbirt KK, Whitmarsh AJ, Davis RJ, Bonkovsky HL. Mechanism of sodium arsenite-mediated induction of heme oxygenase-1 in hepatoma cells. Role of mitogen-activated protein kinases. J Biol Chem 1998; 273: 8922-8931.

[30] Bauman JW, Liu J, Klaassen CD. Production of metallothionein and heat-shock proteins in response to metals. Fundam Appl Toxicol 1993; 21: 15-22.

[31] Yoshioka T, Bills T, Moore-Jarrett T, Greene HL, Burr IM, Ichikawa I. Role of intrinsic antioxidant enzymes in renal oxidant injury. Kidney Int 1990; 38: 282-288.

[32] Lai CC, Peng M, Huang L, Huang WH, Chiu TH. Chronic exposure of neonatal cardiac myocytes to hydrogen peroxide enhances the expression of catalase. J Mol Cell Cardiol 1996; 28: 1157-1163.

[33] Clerch LB, Iqbal J, Massaro D. Perinatal rat lung catalase gene expression: influence of corticosteroid and hyperoxia. Am J Physiol 1991; 260: L428-433.

[34] Nath KA, Croatt AJ, Likely S, Behrens TW, Warden D. Renal oxidant injury and oxidant response induced by mercury. Kidney Int 1996; 50: 1032-1043.

[35] Ohtake T, Kimura M, Nishimura M, Hishida A. Roles of reactive oxygen species and antioxidant enzymes in murine daunomycin-induced nephropathy. J Lab Clin Med 1997; 129: 81-88.

[36] Iqbal M, Athar M. Attenuation of iron-nitrilotriacetate (Fe-NTA)-mediated renal oxidative stress, toxicity and hyperproliferative response by the prophylactic treatment of rats with garlic oil. Food Chem Toxicol 1998; 36: 485-495.

[37] Kinter M, Wolstenholme JT, Thornhill BA, Newton EA, McCormick ML, Chevalier RL. Unilateral ureteral obstruction impairs renal antioxidant enzyme activation during sodium depletion. Kidney Int 1999; 55: 1327-1334.

[38] Nath KA, Grande J, Croatt A, Haugen J, Kim Y, Rosenberg ME. Redox regulation of renal DNA synthesis, transforming

growth factor-beta1 and collagen gene expression. Kidney Int 1998; 53: 367-381.

[39] Clerch LB, Wright A, Chung DJ, Massaro D. Early divergent lung antioxidant enzyme expression in response to lipopolysaccharide. Am J Physiol 1996; 271: L949-954.

[40] Singh I, Gulati S, Orak JK, Singh AK. Expression of antioxidant enzymes in rat kidney during ischemia-reperfusion injury. Mol Cell Biochem 1993; 125: 97-104.

[41] Cvetković T, Vlahović P, Pavlović D, Kocić G, Jevtović T, Djordjević VB. Low catalase activity in rats with ureteral ligation: relation to lipid peroxidation. Exp Nephrol 1998; 6: 74-77.

[42] Ricardo SD, Ding G, Eufemio M, Diamond JR. Antioxidant expression in experimental hydronephrosis: role of mechanical stretch and growth factors. Am J Physiol 1997; 272: F789-798.

[43] Cao C, Leng Y, Kufe D. Catalase activity is regulated by c-Abl and Arg in the oxidative stress response. J Biol Chem 2003; 278: 29667-29675.

[44] Iwai K, Kondo T, Watanabe M, Yabu T, Kitano T, Taguchi

Y, Umehara H, Takahashi A, Uchiyama T, Okazaki T. Ceramide increases oxidative damage due to inhibition of catalase by caspase-3-dependent proteolysis in HL-60 cell apoptosis. J Biol Chem 2003; 278: 9813-9822.

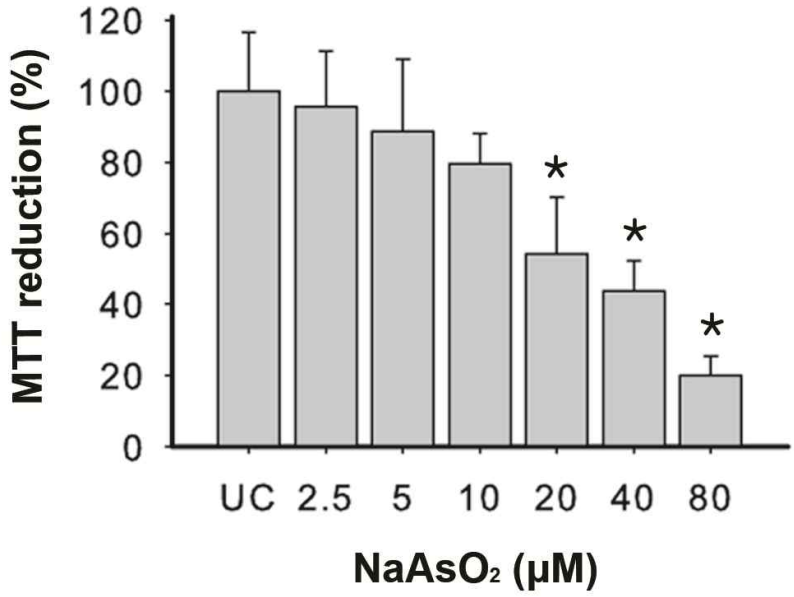

Figure 1. Dose-Dependent Cytotoxicity of Arsenite in HepG2 Cells

HepG2 cells were treated with arsenite at the indicated concentrations for 24 h and cell viability was determined by measuring MTT reduction. The data are expressed as a percentage of reduction values of untreated controls (UC). Data represent mean±S.D. (n=3—5), and asterisks (*) indicate a significant difference compared to UC (p<0.05).

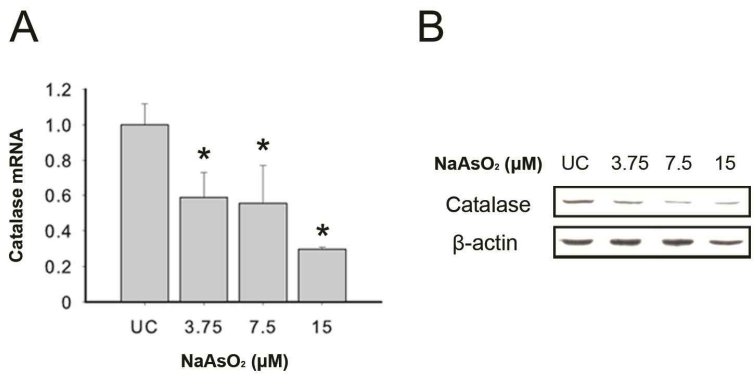

Figure 2. Expression of Catalase in HepG2 Cells Treated with Arsenite

(A) Real-time RT-PCR analysis of catalase mRNA levels in HepG2 cells treated with arsenite at the indicated concentrations for 24 h. The level of catalase mRNA is normalized to β-Actin and expressed in arbitrary units relative to UC (given a value of 1). Data represent mean$\pm$S.D. (n=3—5), and asterisks (*) indicate a significant difference compared to UC (p<0.05). (B) Western blotting analysis of catalase in HepG2 cells treated with arsenite at the indicated concentrations for 24 h. β-Actin was used as internal control.

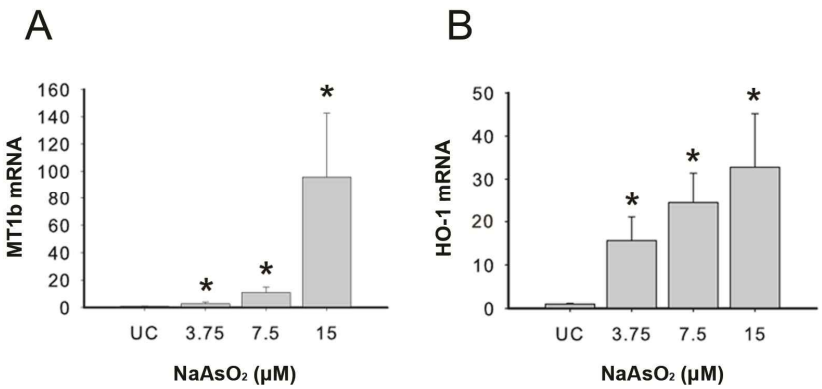

Figure 3. Expression of Oxidative Stress-Responsive MT1b (A) and HO-1 (B) mRNA in HepG2 Cells Treated with Arsenite Levels of mRNA are normalized to β-Actin and expressed in arbitrary units relative to UC (given a value of 1). Data represent mean±S.D. (n=3—5), and asterisks (*) indicate a significant difference compared to UC (p <0.05).

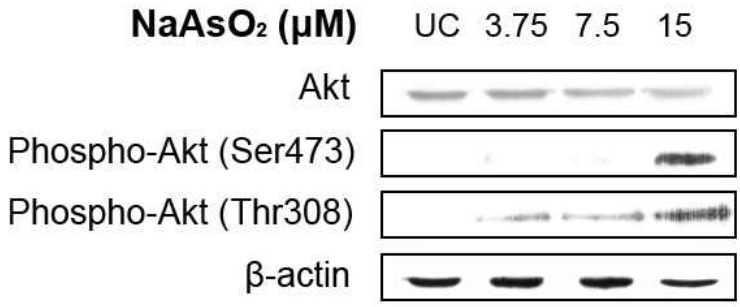

Figure 4. Expression of Total Akt, Phospho-Akt (Ser473) and Phospho-Akt (Thr308) in HepG2 Cells Treated with Arsenite at the Indicated Concentrations for 24 h

The phosphorylation of Akt at residues Ser473 and Thr308 was detected using phopho-Akt-specific antibodies. β-Actin was used as the internal control.

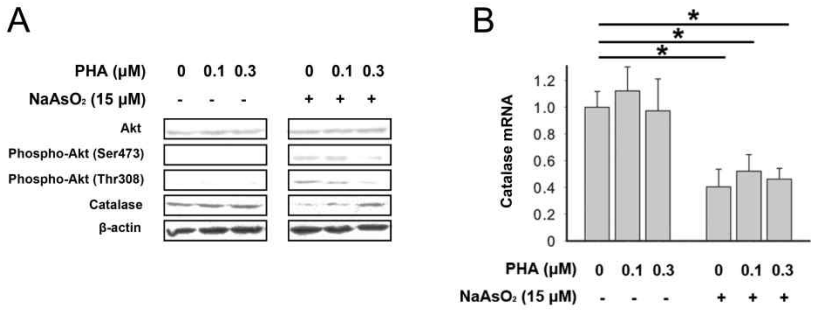

Figure 5. Effect of a c-Met Inhibitor on the Expression of Catalase in HepG2 Cells Treated with Arsenite

HepG2 cells were treated with the indicated concentrations of PHA for 4 h and then with 15 μM arsenite for 24 h. (A) Western blot analysis of total Akt, phospho-Akt (Ser473), phospho-Akt (Thr308) and catalase. β-Actin was used as internal control. (B) Real-time RT-PCR analysis of catalase mRNA levels. The level of catalase mRNA is normalized to β-Actin and expressed in arbitrary units relative to the untreated group (given a value of 1). Data represent mean$\pm$S.D. (n=3—5), and asterisks (*) indicate a significant difference (p<0.05) between the two treatment groups.

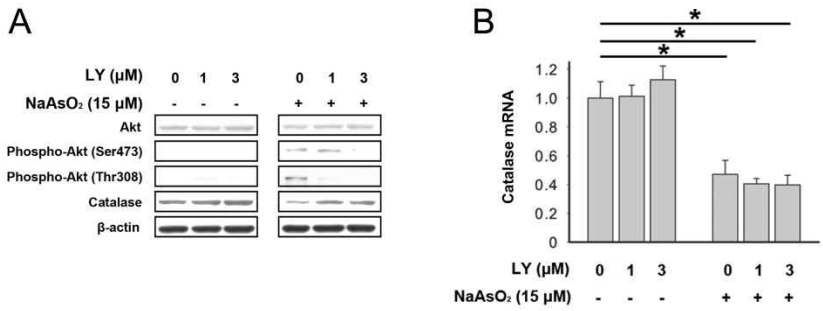

Figure 6. Effect of a PI3K Inhibitor on the Expression of Catalase in HepG2 Cells Treated with Arsenite

HepG2 cells were co-treated with the indicated concentrations of LY and 15 μM arsenite for 24 h. (A) Western blot analysis of total Akt, phospho-Akt (Ser473), phospho-Akt (Thr308) and catalase. β-Actin was used as internal control. (B) Real-time RT-PCR analysis of catalase mRNA levels. The level of catalase mRNA is normalized to β-Actin and expressed in arbitrary units relative to the untreated group (given a value of 1). Data represent mean$\pm$S.D. (n=3—5), and asterisks (*) indicate a significant difference (p<0.05) between the two treatment groups.

Table 1. Primer Sets Employed in Real-Time RT-PCR Analysis

mRNA	Accession #[a]	Primer sequence (5'→ 3')
β-Actin	NM_001101.3	Forward : GCTCCTCCTGAGCGCAAG Reverse : CATCTGCTGGAAGGTGGACA
Catalase	NM_001752.3	Forward : ACATGGTCTGGGACTTCTGG Reverse : CTTGGGTCGAAGGCTATCTG
HO-1	NM_002133.2	Forward : AACTTTCAGAAGGGCCAGGT Reverse : AGCTGGATGTTGAGCAGGA
MT1b	NM_005947.2	Forward : GCAAGAAGTGCTGCTGCTCTT Reverse : TCTGATGAGCCTTTGCAGACA

a) GenBank accession numbers (http://www.ncbi.nlm.nih.gov).

CHAPTER Ⅲ

HIGH-DOSE ARSENIC TRIOXIDE-INDUCED APOPTOSIS THROUGH AKT-DEPENDENT ACTIVATION OF GSK3 β

1. Introduction

Arsenic is known as both a carcinogen and an anticancer agent [1]. Arsenic has been generally considered a potent human carcinogen based on the epidemiological studies, which showed a relationship between inorganic arsenic in drinking water and increased risk of skin cancer. However, arsenic trioxide (ATO) was reported to induce remission in patients with acute promyelocytic leukemia (APL) in China in the 1970s [2, 3]. The anti-cancer efficiency of ATO was not restricted to APL; rather, it has been extended to many solid tumors, including liver, cervical, prostate, lung, esophagus, and bladder tumors [4-7].

The mechanism of the carcinogenic or anticancer activity of ATO is complicated, and various effects are observed depending on the applied concentration of ATO. Low concentrations can induce differentiation or cell cycle arrest, whereas high concentrations can induce apoptosis [8]. An in vitro study has shown that high concentration of ATO inhibit growth and promote apoptosis in many different cancer cell lines, including colon cancer cells and hepatoma cells [5, 9, 10]. Although several mechanisms have emerged that appear to be commonly associated with ATO-induced apoptosis, reactive oxygen species (ROS)-mediated oxidative damage is considered a common denominator in apoptosis [11, 12].

The biological effects of arsenic may be attributed to structural and functional alterations of critical cellular proteins, due to its reactivity with sulfhydryl groups [13]. The resulting loss of specific enzymes, including kinases and phosphatases, functionally alters diverse signaling pathways and the degradation of specific proteins involved in pro-survival pathways [8].

Phosphatidylinositol 3-kinase (PI3K)/Akt is thought to play a pivotal role in regulating cell survival [14]. Previous studies have shown that the PI3K/Akt pathway contributes to tumorigenesis, metastasis, and resistance to chemotherapy by modulating the function of numerous substrates, including BAD, CREB, mTOR, and GSK3β [15-19]. For this reason, the PI3K/Akt signaling pathway is considered a cancer therapeutic target [20]. Supporting this, the PI3K inhibitors LY294002 (LY) and wortmannin were observed to exert antitumor activity and enhance apoptosis [17, 19, 21].

Some studies suggest that arsenic inactivates Akt-related cell survival pathways. In NB4 human APL cells, for example, ATO decreased not only Akt activity, but also total Akt protein, leading to the induction of apoptosis [22]. ATO-induced inactivation of Akt has also been demonstrated in gallbladder carcinoma cells [23] and ovarian cancer cells [24].

In this study, we investigated the mechanism of ATO-induced cell death through inhibition of both Akt1 expression

and phosphorylation in human cancer cell lines. Further examination of the signaling pathways indicated that GSK3β, a ubiquitously expressed protein-serine/threonine kinase, is a critical downstream substrate of the Akt cell survival pathway [25, 26] involved in ATO-induced apoptosis. The results showed that Akt1-mediated GSK3β activation could be a mechanism of ATO-induced cell death in human hepatoma HepG2 cells.

2. Material and methods

2.1. Materials

Human hepatoma (HepG2) cells, human colon cancer (HCT116) cells, human cervical cancer (HeLa) cells and human prostatic carcinoma (PC3) cells were obtained from the Korean Cell Line Bank (KCLB, Seoul, Korea).

All chemicals were reagent grade or higher and were obtained from Sigma-Aldrich (St. Louis, MO), unless otherwise specified. Fetal bovine serum was purchased from Gibco (Grand Island, NY). PI3K inhibitor, LY was purchased from BioVision (Mountain View, CA). Trizol reagent, reverse transcriptase, and transfection reagents were purchased from Invitrogen (Carlsbad, CA). Apoptosis detection Kit (Annexin

V-FITC) and InstantOneTM ELISA kit (Akt pathway activation) were purchased from BD Pharmingen (San Diego, CA) and purchased from eBioscience (San Diego, CA), respectively.

2.2. Cell treatment and cell viability assay

HepG2 cells, HCT116 cells, HeLa cells and PC3 cells were grown in RPMI 1640 media with 2 mg/mL sodium bicarbonate, 25 mM HEPES, 10% (v/v) fetal bovine serum, 100 unit/mL penicillin, and 100 μg/mL streptomycin. The cells were maintained at 37°C in a 5% CO2 incubator. Twenty-four hours after the cells were plated, the culture medium was removed and replaced with medium containing various concentrations of ATO (A1010), Triton X-100 (Triton, T9284) and sodium dodecyl sulfate (SDS, 71736). For the antioxidant and the PI3K inhibition studies, HepG2 cells were treated with antioxidant for 2 h followed by ATO for 24 h, and co-treated with LY and ATO for 24 h, respectively.

MTT (3-(4,5-dimethylthiazol-2-yl)-2,5-diphenyl tetrazolium bromide) reduction was used as parameters for cell viability assessment. MTT reduction was examined according to the methods of Mosmann [27], with modification. Briefly, 10× MTT stock solution (5 mg/mL in phosphate buffered saline (PBS), pH 7.4) was added to each culture well,

and the plates were incubated at 37℃ for 2 h. The MTT solution was then aspirated, and 0.2 ml of acidified isopropanol (0.04 N HCl in isopropanol) was added to each well to dissolve the formazan. After a few minutes at room temperature, the plates were read on a microplate reader (Molecular Devices, Sunnyvale, CA) at a wavelength of 560 nm.

2.3. Real time reverse transcriptase polymerase chain reaction (RT-PCR)

Total RNA was extracted from cells using Trizol reagent according to the manufacturer's instructions. The amount of RNA in each sample was quantified using a Nanodrop ND-1000 spectrophotometer (NanoDrop Technologies, Wilmington, DE), and 0.5 μg of total RNA was reverse transcribed using reverse transcriptase and random hexamers. Then real-time RT-PCR was performed with cDNAs and gene-specific primers (Table 1, Bioneer, Daejeon, Korea) using ABI SYBR Green PCR master mix (Applied Biosystems, Foster City, CA) in an ABI Prism 7000 thermocycler (Applied Biosystems). Samples were first denatured for 10 min at 95℃ and then the amplification and quantification program was repeated 40 times (15 s at 95℃, 1 min at 60℃). This

program was followed by a melting curve program (60–99°C with a heating rate of 0.1°C/s and continuous fluorescence measurement).

2.4. Western blot

Samples containing 20 μg of proteins extracted from cells were denatured by boiling for 10 min in 5× SDS gel loading buffer (5% SDS; 0.225 M Tris, pH 6.8; 50% glycerol; 0.05% bromophenol blue; 0.25 M dithiothreitol), separated by SDS–polyacrylamide gel electrophoresis, and then transferred to nitrocellulose membranes. The blots were blocked by incubation with 5% skim milk for 1 h and then incubated with anti–akt1 (sc–5298, Santa Cruz Biotechnology, Santa Cruz, CA), anti–Bcl2 (sc492, Santa Cruz Biotechnology), anti GSK3β (sc–9166, Santa Cruz Biotechnology) and anti–β–actin (A5441) overnight at 4℃. The blots were then incubated with horse–radish peroxidase (HRP)–conjugated Immunoglobulin G (IgG) as secondary antibody and developed with chemiluminescence reagents (Ab Frontier, Seoul, Korea). HRP–conjugated goat anti–mouse IgG (SA001–500) and HRP–conjugated goat anti–rabbit IgG (SA002–500) were purchased from GenDepot (Barker, TX). The Western blot procedure provides a qualitative, not quantitative, comparison between samples; therefore, no

statistical analysis was performed.

2.5. Annexin V-FITC analysis

HepG2 cells were plated as described above and then incubated with N-acetylcysteine (NAC) for 2 h before challenge with ATO for 24 h. Cells were harvested, washed twice with PBS and centrifuged. Cells were labeled by incubation with Annexin V-FITC in a binding buffer for 15 min at RT in the dark. Stained cells were analyzed using BD FACSAria II cell sorter with BD FACS Diva software (Becton Dickinson, Franklin Lakes, NJ).

2.6. Phosphrylated Akt and GSK3β Enzyme-Linked Immunosorbent Assay (ELISA)

The AKT Pathway Activation Profile InstantOneTM ELISA kit was used to measure levels of phosphorylated Akt (Ser473), GSK3β (Ser9) and p70S6K (Thr 389) in HepG2 cells according to the instruction manual. After treatment, cell lysate (total protein 100 μg) were incubated for 1 h with the antibody cocktail for p-Akt, p-GSK3β and p-p70S6K. The wells were washed three times with 1× wash buffer and the color was developed by adding 100 μL of detection reagent

and incubating the plates in dark for 10 min. The reaction was stopped using 100 μL of stop solution and the plated were read on a microplate reader (Molecular Devices) at a wavelength of 450 nm.

2.7. Plasmid and RNAi transfection

Transfection was achieved on day 1 after plating of cells in 6 well plates with a confluence of 70–80% at the time of transfection. Transient plasmid transfection for ectopic Bcl2 expression in HepG2 was performed using lipofectamine LTX and PLUS reagents in OptiMEM® according to the instruction manual. HepG2 cells were transfected with pcDNA3-Bcl2 (#3336, addgene, Cambridge, MA) or pcDNA3 for 72 h. Transfection efficiency was evaluated by western blot after transfection.

Transient knockdown of GSK3β was achieved in HepG2 cells using siRNA (s6239, #4390824, Ambion, Austin, TX). Unrelated control siRNA (#4390843, Ambion) was also used. HepG2 cells were transfected in OptiMEM® using RNAiMAX™ for 72 h according to the manufacturer's protocol.

2.8. Statistical analysis

All data are expressed as mean ± standard deviation (S.D.). The Mann–Whitney test was performed to compare selected pairs of groups (SAS 9.13 statistical program, SAS Institute, Cary, NC), and a P−value less than 0.05 was considered significant. The IC50 value, corresponding to the concentration producing a 50% inhibition of cell viability, was determined by probit analysis (Biostat 2009, AnalystSoft, Vancouver, Canada).

3. Results

3.1. Inhibitory effects of ATO on Akt1 expression

Expression of Akt1 mRNA and protein was analyzed in HepG2 (Figure 1A), HCT116 (Figure 1B), HeLa (Figure 1C), and PC3 cells (Figure 1D) treated for 24 h with 15 or 30 μM ATO. MTT reduction was used to study the effects of ATO on cell viability, and the concentration of ATO used in the cellular treatment was based on the IC50. The IC50 in HepG2, HCT116, HeLa, and PC3 cells treated with ATO for 24 h was 40.75 ± 1.69, 44.33 ± 2.98, 24.64 ± 8.16, and 33.53 ± 7.41 μM, respectively. The mRNA level of Akt1 decreased significantly in all four cancer cell lines after 24 h treatment with 30 μM ATO. Akt1 mRNA expression was also decreased

significantly 24 h after treatment with 15 μM ATO in HeLa cells (Fig 1C). We also analyzed the abundance of Akt1 protein in HepG2, HCT116, HeLa, and PC3 cells treated with two different concentrations of ATO by western blot (Figure 1A, B, C, and D). Similar to the Akt1 mRNA expression, the protein level of Akt1 dose-dependently decreased in all four cell lines after 24 h treatment with ATO.

In addition, the effects of cytotoxic agents that damage cell membranes, such as Triton (Figure 1E) and SDS (Figure 1F), on Akt1 expression were studied in HepG2 cells. The concentration of Triton and SDS used in the cellular treatment was based on the IC50, 0.0032 ± 0.0003% and 0.0065 ± 0.0011%, respectively. Akt1 mRNA and protein expression were not changed significantly in HepG2 cells treated with Triton and SDS for 24 h.

3.2. Effect of antioxidants on ATO-derived Akt1 inhibition

NAC, which serves as a precursor for the synthesis of glutathione, and ascorbic acid (AA), which interacts directly with the oxidizing radicals, are important antioxidants. The protective effect of antioxidants against ATO activity was demonstrated using an MTT assay (data not shown). ATO-

induced inhibition of Akt1 mRNA expression was significantly abolished by NAC (Figure 2A) and AA (Figure 2B). Further, the Akt1 mRNA and protein expression in HepG2 cells pretreated with 10 mM NAC or 1 mM AA for 2 h before ATO challenge (24 h) was nearly equivalent to ATO-untreated controls (Figure 2A, B, and C).

To further investigate the mechanism of ATO-induced cell death, Annexin V-FITC staining was performed by flow cytometry after treatment of HepG2 cells with 15 or 30 μM ATO for 24 h. ATO dose-dependently induced Annexin V-FITC positive staining in HepG2 cells, indicating that ATO induced apoptosis (Figure 2D). However, the induction of apoptosis was prevented by pre-treatment of the cells with 10 mM NAC for 2 h.

3.3. Effect of ectopic Bcl2 expression on the levels of Akt1

Because Bcl2 is known to play an important role in the apoptosis, we transiently overexpressed Bcl2 in HepG2 cells to identify a possible mechanism underlying ATO-induced apoptosis. Transient transfection with Bcl2 increased Bcl2 protein expression and suppressed the inhibitory effects of ATO on Akt1 expression in HepG2 cells (Fig 3A). To

investigate whether overexpression of Bcl2 and Akt is involved in ATO-induced cell death, the effect of the PI3K/Akt inhibitor LY on Bcl2-overexpressing cells treated with ATO was examined (Fig 3B). LY treatment attenuated the effects of ectopic Bcl2 expression on cell viability in HepG2 cells treated with ATO up to 60 μM for 24 h.

3.4. Akt pathway activation and role of GSK3β in HepG2 cells treated with ATO

To determine whether the Akt pathway is inactivated in HepG2 cells after treatment with ATO, phosphorylation of Akt at Ser473, GSK3β at Ser9, and p70S6K at Thr389 was examined. As shown in Figure 4, constitutive phosphorylation of Akt, GSK3β and p70S6K was seen in HepG2 cells lines, and phosphorylation was decreased in a dose-dependent manner after 24 h treatment with ATO, similar to the Akt1 mRNA and protein expression. To further confirm the role of GSK3β in ATO-mediated cytotoxicity, HepG2 cells were transiently transfected with GSK3β siRNA for 72 h and subsequently treated with ATO for another 24 h. First, the specific knockdown of GSK-3β expression and phosphorylation were confirmed using western blot analysis and ELISA (Figure 5A and B). GSK3β knockdown did not alter the downregulation of Akt1 compared to cells

transfected with control siRNA after ATO treatment (24 h). Additionally, we did not observe significant changes in the inhibition of GSK3β phosphorylation in HepG2 cells transfected with GSK3β siRNA compared to cells transfected with control siRNA after treatment with ATO for 24 h (Figure 5B). In contrast, GSK3β siRNA-transfected cells, were resistant to apoptosis after treatment with ATO, as compared to cells expressing a control siRNA. These results indicated that ATO predominantly affects unphosphorylated (activated) GSK3β by inhibiting AKT-mediated phosphorylation, which was demonstrated by the GSK3β knockdown (Figure 5C).

4. Discussion

In the present study, ATO-induced apoptosis in human hepatoma cells and its underlying molecular mechanisms were investigated. Our results showed that ATO induced apoptosis via the inactivation of Akt and enhanced ROS production, which was prevented by antioxidants. Furthermore, Bcl-2 overexpression and GSK3β silencing attenuates ATO-induced apoptosis.

ATO is used to treat patients with APL, and it anti-cancer efficacy has been extended to solid tumors, including hepatocellular carcinomas [10, 28-30]. Several previous studies have reported that ATO exhibits anti-cancer activity

through the induction of apoptosis in various solid tumor cells lines, including hepatocellular carcinoma cells, ovarian cancer cells, colon cancer cells, and gallbladder carcinoma cells [9, 23, 28, 31]. An in vivo study has also assessed the effects and efficacy of ATO on gastrointerstinal cancer cell apoptosis by administering ATO to gastrointestinal cancer patients [32]. However, its activity against solid tumors seems less effective than against APL, because the doses required to exert anti-cancer effects on solid tumors are much higher than those required for hematologic malignancies [28, 29, 30, 33]. High doses are not clinically achievable without the risk of severe side-effects and toxicity. Recently, a phase II trial evaluating the efficacy and toxicity of single-agent ATO in patients with hepatocellular carcinoma reported that single-agent ATO has poor efficacy against advanced hepatocellular carcinoma [34]. New strategies to enhance the efficacy of ATO while reducing the dose of ATO to avoid the severe side-effects are essential for the treatment of hepatocellular carcinoma. In the current study, we used relatively high concentrations over a longer time-period (24 h) to inhibit human cancer cell line viability, including HepG2, HCT116, HeLa, and PC3 cells (Figure 1). Therefore, understanding the mechanisms by which ATO induce apoptosis may identify potential targets for combination therapies and broaden the malignancies for which arsenic can provide effective

treatment.

Oxidative damage has been postulated to play a key role in ATO-induced apoptosis [9, 11]. The present study also showed that ATO-induced apoptosis and inhibition of Akt was mediated by ROS, and is prevented by antioxidants, such as NAC and AA (Figure 2). Since ROS elevation has been reported to sensitize leukemic cells to ATO-induced apoptosis [35], and that treatment with H2O2 resulted in proteolysis of Akt [36], ROS may trigger ATO-induced apoptosis and the inhibition of Akt.

The PI3K/Akt signaling pathway is involved in cell survival and growth [37]. A previous study indicated that Akt1 kinase is frequently activated in human cancer, and is considered a potential target for cancer intervention [38]. The results of this study showed that ATO inhibited the mRNA expression, protein expression, and activation of Akt1 in HepG2 cells (Figure 1 and 4). Although Akt phosphorylates a number of downstream targets, this study identified that GSK3β is responsible for ATO-induced apoptosis in HepG2 cells. GSK3β is a primary target of Akt, which inactivates GSK3β function by phosphorylation. GSK3β was initially described as an enzyme involved in glycogen metabolism, but is also known to regulate a diverse array of cell functions [39, 40]. Recent studies have characterized GSK3β as being closely associated with apoptosis. To confirm that approach in

our study, GSK3β was suppressed by a GSK3β-specific siRNA. We demonstrated that GSK3β downregulation by RNAi did not alter Akt1 expression and GSK3β phosphorylation by ATO (Figure 5). Our results suggest that non-phosphorylated GSK3β is required for ATO-induced apoptosis. Suppression of Akt expression by ATO contributed to decreased Akt phosphorylation and activation of GSK3β. Consistent with this study, overexpression of GSK3β induced apoptosis in pheochromocytoma cells [26].

In addition, Bcl2 plays a role in neoplasia by inhibition of tumor cell apoptosis [41]. Ai et al. [23] and Ma et al. [32] have reported an ATO-induced downregulation of Bcl2 in gallbladder carcinoma cells and gastrointestinal cancer cells, respectively. To determine the contribution of Bcl2 to ATO-induced apoptosis, we examined the effect of overexpression of Bcl2 in ATO-treated HepG2 cells. However, the effect of ATO on Bcl2 expression in HepG2 cells was not determined in this study. Instead, overexpression of Bcl2 blocked ATO-induced apoptosis, whereas LY attenuated the effects of Bcl2 expression, demonstrating that suppression of PI3K/Akt activation enhances ATO-induced apoptosis (Figure 3).

In summary, we demonstrated that ATO induced apoptosis by the PI3K/Akt/GSK3β pathway in human hepatoma cells. Suppression of Akt expression led to decreased Akt phosphorylation followed by GSK3β activation.

Our finding improves the understanding of the PI3K/Akt/GSK3β signaling pathway in human cancer, and identifies GSK3β as a novel target to facilitate the anti-tumorigenic activity of ATO. Additional work will be required to evaluate other factors involved in ATO-induced cell death and focus on identifying the substrates of GSK3β to further understand how ATO exhibits anti-carcinogenic activity in solid tumors. The combined treatment with a GSK3β activator may increase the therapeutic efficacy of arsenic. A comprehensive study on the biology of ATO will help in developing ATO-based therapeutic interventions for hepatic carcinoma.

5. References

[1] Cui X, Kobayashi Y, Akashi M, Okayasu R. Metabolism and the paradoxical effects of arsenic: carcinogenesis and anticancer. Curr Med Chem 2008; 15: 2293-2304.

[2] Shen ZX, Chen GQ, Ni JH, Li XS, Xiong SM, Qiu QY, Zhu J, Tang W, Sun GL, Yang KQ, Chen Y, Zhou L, Fang ZW, Wang YT, Ma J, Zhang P, Zhang TD, Chen SJ, Chen Z, Wang ZY. Use of arsenic trioxide (As2O3) in the treatment of acute promyelocytic leukemia (APL): II. Clinical efficacy and pharmacokinetics in relapsed patients. Blood 1997; 89: 3354-

3360.

[3] Rossman TG. Mechanism of arsenic carcinogenesis: an integrated approach. Mutat Res 2003; 533: 37-65.

[4] Diepart C, Karroum O, Magat J, Feron O, Verrax J, Calderon PB, Grégoire V, Leveque P, Stockis J, Dauguet N, Jordan BF, Gallez B. Arsenic trioxide treatment decreases the oxygen consumption rate of tumor cells and radiosensitizes solid tumors. Cancer Res 2012; 72: 482-490.

[5] Murgo AJ. Clinical trials of arsenic trioxide in hematologic and solid tumors: overview of the National Cancer Institute Cooperative Research and Development Studies. Oncologist 2001; 2: 22-28.

[6] Maeda H, Hori S, Nishitoh H, Ichijo H, Ogawa O, Kakehi Y, Kakizuka A. Tumor growth inhibition by arsenic trioxide (As2O3) in the orthotopic metastasis model of androgen-independent prostate cancer. Cancer Res 2001; 61: 5432-5440.

[7] Yu J, Qian H, Li Y, Wang Y, Zhang X, Liang X, Fu M, Lin C. Arsenic trioxide (As2O3) reduces the invasive and metastatic properties of cervical cancer cells *in vitro* and *in vivo*.

Gynecol Oncol 2007; 106: 400-406.

[8] Mathas S, Lietz A, Janz M, Hinz M, Jundt F, Scheidereit C, Bommert K, Dorken B. Inhibition of NF-kappaB essentially contributes to arsenic-induced apoptosis. Blood 2003; 102: 1028-1034.

[9] Nakagawa Y, Akao Y, Morikawa H, Hirata I, Katsu K, Naoe T, Ohishi N, Yagi K. Arsenic trioxide-induced apoptosis through oxidative stress in cells of colon cancer cell lines. Life Sci 2002; 70: 2253-2269.

[10] Oketani M, Kohara K, Tuvdendorj D, Ishitsuka K, Komorizono Y, Ishibashi K, Arima T. Inhibition by arsenic trioxide of human hepatoma cell growth. Cancer Lett 2002; 183: 147-153.

[11] Jomova K, Jenisova Z, Feszterova M, Baros S, Liska J, Hudecova D, Rhodes CJ, Valko M. Arsenic: toxicity, oxidative stress and human disease. J Appl Toxicol 2011; 31: 95-107.

[12] Liu L, Trimarchi JR, Navarro P, Blasco MA, Keefe DL. Oxidative stress contributes to arsenic-induced telomere attrition, chromosome instability and apoptosis. J Biol Chem 2003; 278: 31998-32004.

[13] Snow ET. Metal carcinogenesis: mechanistic implications. Pharmacol Ther 1992; 53: 31-65.

[14] Datta SR, Brunet A, Greenberg ME. Cellular survival: a play in three Akts. Genes Dev 1999; 13: 2905-2927.

[15] Lou J, Manning BD, Cantley LC. Targeting the PI3K-Akt pathway in human cancer-Rationale and promise. Cancer cell 2003; 4: 257-262.

[16] Testa JR, Bellacosa A. AKT plays a central role in tumorigenesis. Proc Natl Acad Sci USA 2001; 98: 10983-10985.

[17] Fresno Vara JA, Casado E, de Castro J, Cejas P, Belda-Iniesta C, González-Barón M. PI3K/Akt signalling pathway and cancer. Cancer Treat Rev 2004; 30: 193-204.

[18] Gao Q, Liu H, Yao Y, Geng L, Zhang X, Jiang L, Shi B, Yang F. Carnosic acid induces autophagic cell death through inhibition of the Akt/mTOR pathway in human hepatoma cells. J Appl Toxicol 2015; 35: 485-492.

[19] West KA, Castillo SS, Dennis PA. Activation of the

PI3K/Akt pathway and chemotherapeutic resistance. Drug Resist Updat 2002; 5: 234-248.

[20] Franke TF, Hornik CP, Segev L, Shostak GA, Sugimoto C. PI3K/Akt and apoptosis: size matters. Oncogene 2003; 22: 8983-8998.

[21] Ng SSW, Tsao MS, Chow S, Hedley DW. Inhibition of phosphatidylinositide 3-kinase enhances gemcitabine-induced apoptosis in human pancreatic cancer cells. Cancer Res 2000; 60: 5451-5455.

[22] Mann KK, Colombo M, Miller WH Jr. Arsenic trioxide decreases AKT protein in a caspase-dependent manner. Mol Cancer Ther 2008; 7: 1680-1687.

[23] Ai Z, Lu W, Qin X. Arsenic trioxide induces gallbladder carcinoma cell apoptosis via downregulation of Bcl-2. Biochem Biophys Res Commun 2006; 348: 1075-1081.

[24] Yuan Z, Wang F, Zhao Z, Zhao X, Qiu J, Nie C, Wei Y. BIM-mediated AKT phosphorylation is a key modulator of arsenic trioxide-induced apoptosis in cisplatin-sensitive and -resistant ovarian cancer cells. PLoS One 2011; 6:e20586.

[25] Welsh GI, Wilson C, Proud CG. GSK3: a SHAGGY frog story. Trends Cell Biol 1996; 6: 274-279.

[26] Pap M, Cooper GM. Role of glycogen synthase kinase-3 in the phosphatidylinositol 3-Kinase/Akt cell survival pathway. J Biol Chem 1998; 273: 19929-19932.

[27] Mosmann T. Rapid colorimetric assay for cellular growth and survival: application to proliferation and cytotoxicity assays. J Immunol Methods 1983; 65: 55-63.

[28] Kito M, Akao Y, Ohishi N, Yagi K, Nozawa Y. Arsenic trioxide-induced apoptosis and its enhancement by buthionine sulfoximine in hepatocellular carcinoma cell lines. Biochem Biophys Res Commun 2002; 291: 861-867.

[29] Luo L, Qiao H, Meng F, Dong X, Zhou B, Jiang H, Kanwar JR, Krissansen GW, Sun X. Arsenic trioxide synergizes with B7H3-mediated immunotherapy to eradicate hepatocellular carcinomas. Int J Cancer 2006; 118: 1823-1830.

[30] Liu B, Pan S, Dong X, Qiao H, Jiang H, Krissansen GW, Sun X. Opposing effects of arsenic trioxide on hepatocellular carcinomas in mice. Cancer Sci 2006; 97: 675-681.

[31] Bornstein J, Sagi S, Haj A, Harroch J, Fares F. Arsenic Trioxide inhibits the growth of human ovarian carcinoma cell line. Gynecol Oncol 2005; 99: 726-729.

[32] Ma ZB, Xu HY, Jiang M, Yang YL, Liu LX, Li YH. Arsenic trioxide induces apoptosis of human gastrointestinal cancer cells. World J Gstroenterol 2014; 20: 5505-5510.

[33] Liu P, Han ZC. Treatment of acute promyelocytic leukemia and other hematologic malignancies with arsenic trioxide: review of clinical and basic studies. Int J Hematol 2003; 78: 32-39.

[34] Lin CC, Hsu C, Hsu CH, Hsu WL, Cheng AL, Yang CH. Arsenic trioxide in patients with hepatocellular carcinoma: a phase II trial. Invest New Drugs 2006; 25: 77-84.

[35] Yi J, Gao F, Shi G, Li H, Wang Z, Shi X, Tang X. The inherent cellular level of reactive oxygen species: one of the mechanisms determining apoptotic susceptibility of leukemic cells to arsenic trioxide. Apoptosis 2002; 7: 209-215.

[36] Martin D, Salinas M, Fujita N, Tsuruo T, Cuadrado A. Ceramide and reactive oxygen species generated by H2O2 induce caspase-3-independent degradation of Akt/protein

kinase B. J Biol Chem 2002; 277: 42943–42952.

[37] Yamaguchi K, Lee SH, Eling TE, Baek SJ. Identification of nonsteroidal anti-inflammatory drug-activated gene (NAG-1) as a novel downstream target of phosphatidylinositol 3-kinase/AKT/GSK-3beta pathway. J Biol Chem 2004; 279: 49617-49623.

[38] Sun M, Wang G, Paciga JE, Feldman RI, Yuan ZQ, Ma XL, Shelley SA, Jove R, Tsichlis PN, Nicosia SV, Cheng JQ. AKT1/PKBalpha kinase is frequently elevated in human cancers and its constitutive activation is required for oncogenic transformation in NIH3T3 cells. Am J Pathol 2001; 159: 431-437.

[39] Doble BW, Woodgett JR. GSK-3: tricks of the trade for a multi-tasking kinase. J Cell Sci 2003; 116: 1175-1186.

[40] Frame S, Cohen P. GSK3 takes centre stage more than 20 years after its discovery. Biochem J 2001; 359: 1-16.

[41] Hockenbery DM, Oltvai ZN, Yin XM, Milliman CL. Korsmeyer SJ. Bcl-2 functions in an antioxidant pathway to prevent apoptosis. Cell 1993; 75: 241-251.

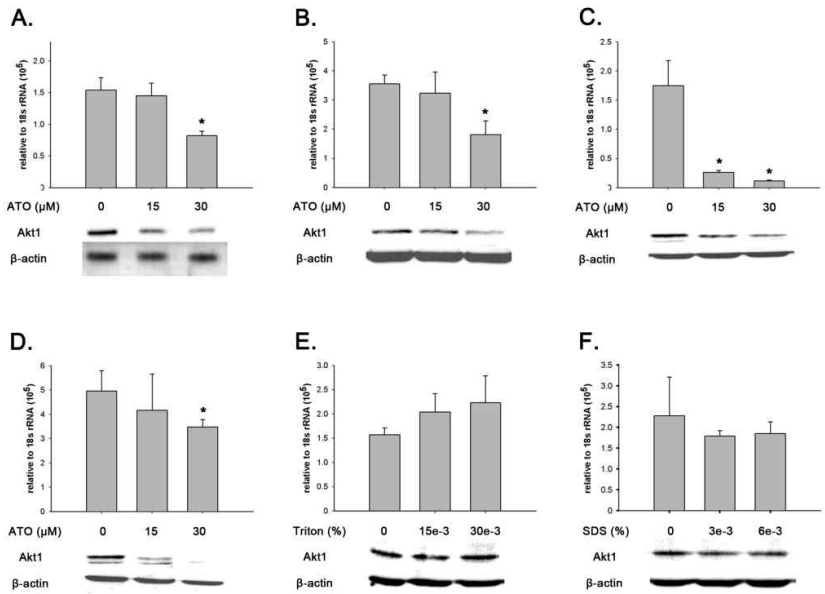

Figure 1. Chemical-dependent inhibitory effects on Akt1 expression in human cancer cell lines. Real time RT-PCR analysis of Akt1 mRNAs and western blotting analysis of Akt1 protein in HepG2 cells (A), HCT116 cells (B), HeLa cells (C) and PC3 cells (D) treated with 15 μM and 30 μM ATO for 24 h. HepG2 cells was also treated with Triton (E) and SDS (F) at the indicated concentrations for 24 h. The level of Akt1 mRNA is normalized to 18s rRNA and β-actin was used as internal control in western blot analysis. Data shown as the mean ± S.D. (n=3-4). *$p<0.05$, compared with ATO-nontreated cells.

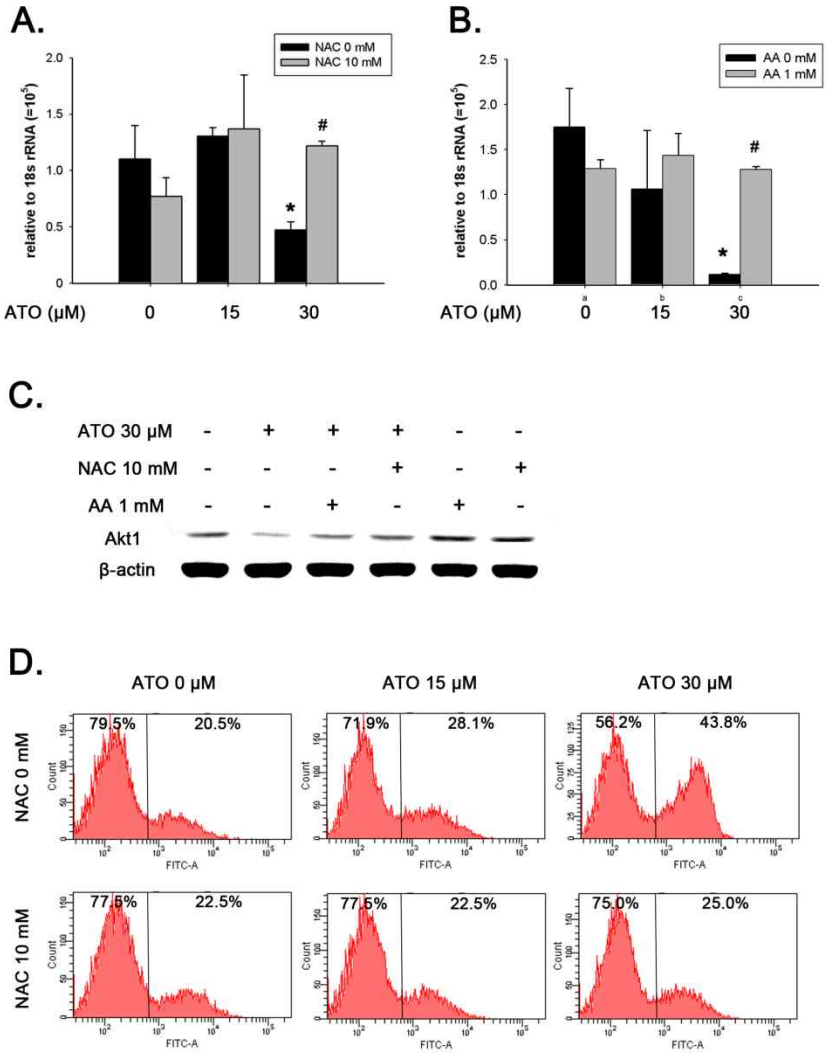

Figure 2. Inhibitory effects of the expression of Akt1 and cell viability in HepG2 cells treated with ATO and its prevention by antioxidant. Real time RT-PCR and western blot analysis of Akt1 expression in HepG2 cells were incubated with NAC (A, C and D) and ascorbic acid (B and C) for 2 h before challenge with ATO for 24 h. For flow cytometry analysis, hepG2 cells were stained with Annexin-V-FITC after ATO treatment (E). The levels of Akt1 mRNA is normalized to 18s rRNA and β-

actin was used as internal control in western blot analysis. Data shown as the mean ± S.D. (n=3-4). *p<0.05, compared with ATO-nontreated cells; #p<0.05, compare to NAC-nontreated cells with ATO at same concentration.

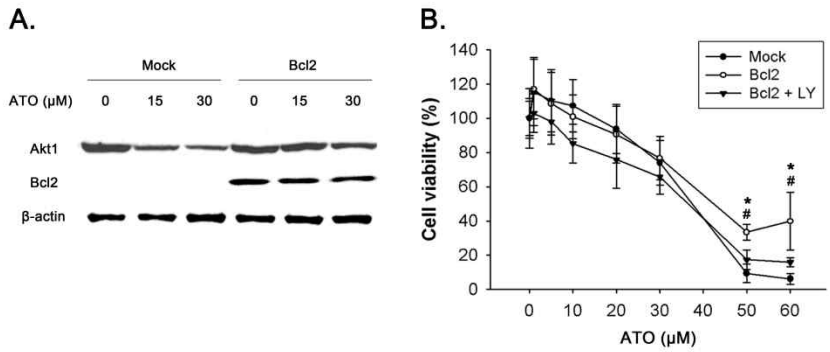

Figure 3. Effects of ectopic Bcl2 expression on the levels of Akt1 and cell viability in HepG2 cells treated with ATO for 24 h. HepG2 cells transiently transfected with PCDNA3/vector (Mock) or PCDNA3/Bcl2 (Bcl2) were subjected to immunoblotting with Akt1 and Bcl2 antibody (A) and cell viability assay determined by measuring MTT reduction (B). Bcl2-overexpressed HepG2 cells were co-treated with the indicated concentrations of ATO and 5 μM LY for 24 h to determine the effect of a PI3K inhibitor on cell viability. β-actin was used as internal control in western blot analysis. Data shown as the mean ± S.D. (n=3-4). *$p<0.05$, compare to Mock transfected cells with ATO at same concentration; #$p<0.05$, compare to LY-nontreated cells with ATO at same concentration in HepG2 cells transfected with Bcl2.

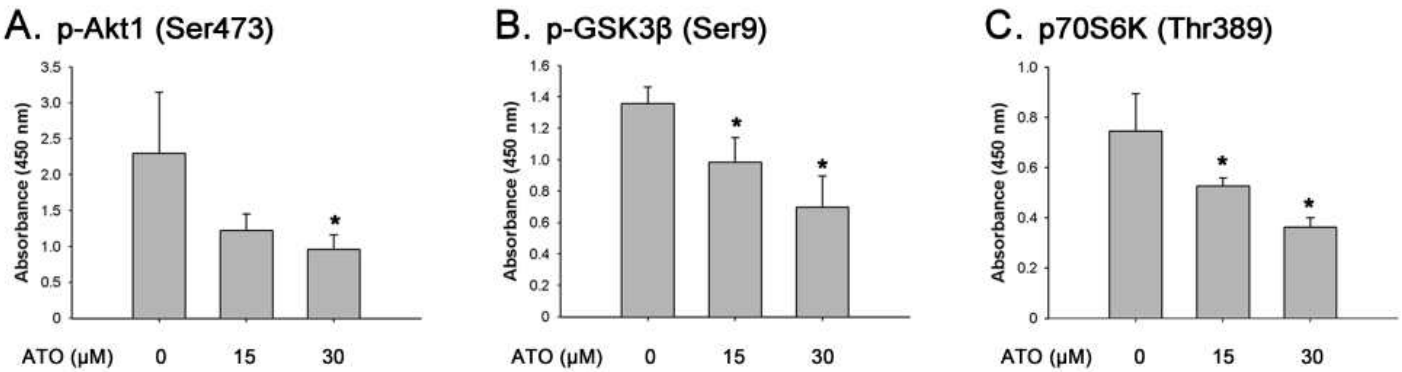

Figure 4. The expression levels of phosphorylated proteins, Akt, GSK3β and p70S6K by treatment with ATO. HepG2 cells were treated with the indicated concentrations of ATO for 24 h. Equal amounts of cell lysates were subjected to ELISA to detect phosphorylation using phospho-Akt, -GSK3β and -p70S6K specific antibodies. Data shown as the mean ± S.D. (n=3-4). *$p<0.05$, compared with ATO-nontreated cells.

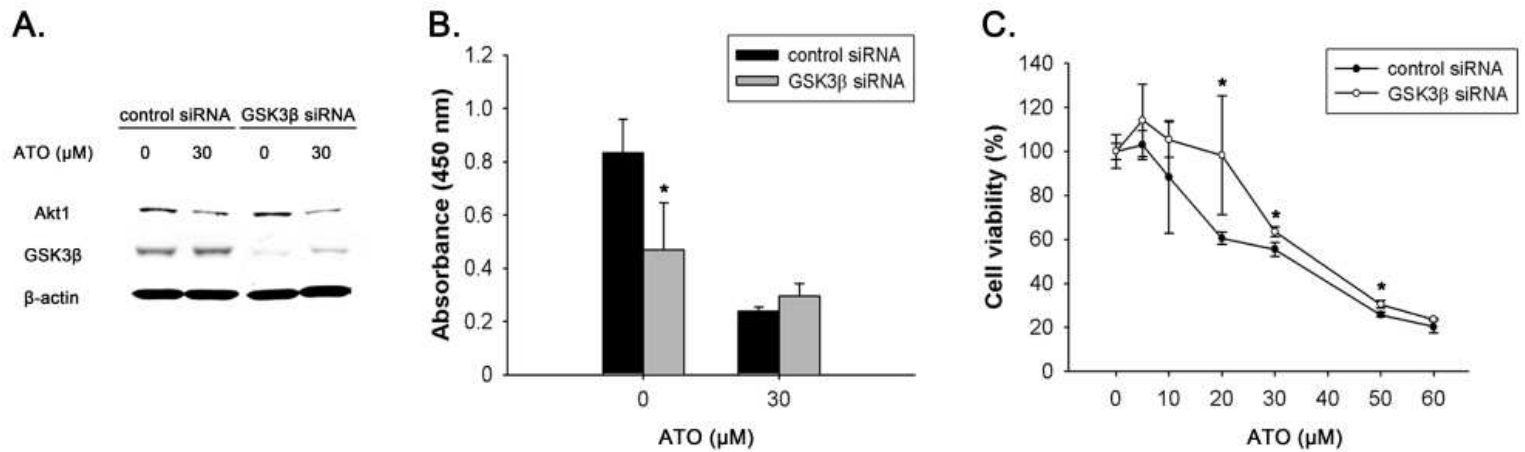

Figure 5. Effects of GSK3β inhibition on the levels of Akt1 and cell viability in HepG2 cells treated with ATO for 24 h. HepG2 cells were transfected with control siRNA and GSK3β siRNA constructs. Seventy-two hours after transfection, cells were treated with 30 μM ATO for 24 h and subject to western blot (A), ELISA using phospho-GSK3β specific antibodies (B) and MTT reduction assay (C). β-actin was used as internal control in western blot analysis. Data shown as the mean ± S.D. (n=3). *$p<0.05$, compared with control siRNA transfected cells with ATO at same concentration.

Table 1. Real time RT-PCR primers

mRNA	Accession # [a]	Forward primer sequence (5′–3′) ; reverse primer sequence (5′–3′)
18S rRNA	NR_003286	TAGAGTGTTCAAAGCAGGCCC ; CCAACAAAATAGAACCGCGGT
Akt1	NM_005163	AGCGACGTGGCTATTGTGAAG ; GCCGCCAGGTCTTGATGTAC

[a] GenBank accession numbers (http://www.ncbi.nlm.nih.gov).

국문초록

세포 및 생체에서의 비소 독성

김수희

서울대학교 대학원

수의병인생물학 및 예방수의학 (환경위생학) 전공

비소는 환경 중에 널리 분포하는 독성 물질로 노출 시 화학적 형태나 농도에 따라 다양한 신호전달체계에 작용한다. 피부, 방광, 폐 등 여러 장기에서 암을 유발하며 당뇨 및 간독성과도 관련이 있다. 비소는 세포의 종류와 화합물의 형태에 따라 세포사멸, 성장억제, 성장 촉진, 발현 억제 등 다양한 반응을 유발한다.

본 연구에서는 비소에 의한 질병 발생 및 치료 기전을 규명하고자 비소에 노출된 영장류 간조직 및 간암유래 세포에서 질병관련 신호전달 체계에 대한 연구를 수행하였다. 먼저 비소에 노출된 영장류 조직에서 추출한 단백질을 프로테오믹스 기법을 이용하여 유의한 발현 변화를 보이는 16개의 단백질을 확인하였다. Mortalin과 tubulin beta chain은 증가를 나머지 14개의 단백질 (plastin-3, cystathionine-beta-synthase, selenium-binding protein 1, annexin A6, alpha-enolase, phosphoenolpyruvate carboxykinase-M, erlin-2, and arginase-1 등) 발현은 비소에 의해 유의한 감소를 보였다. 확인된 16개의 단백질은 대부분

간독성, 세포사멸, 암 발생과 관련이 있었으며, 그 중 4개의 단백질을 선별하여 간암세포주에서 비소에 의한 발현 변화가 유사함을 확인하였다. 또한 비소에 의한 산화적 스트레스, DNA 손상, 당신생 작용기전에 관여하는 단백질의 발현변화를 확인하고, 그 중 간암세포주에서 비소에 의한 catalase 감소와 c-Met/PI3K 신호전달체계와의 관련성에 대한 실험을 추가로 수행하였다. 그 결과, 비소에 의해 활성화된 Akt가 catalase의 발현을 유전자 및 단백질 수준에서 억제하였으며, c-Met과 PI3K의 억제제인 PHA665752와 LY294002를 이용하여 catalase의 전사 후 발현 억제는 c-Met과 PI3K 신호전달체계와 관련이 있다는 것을 알 수 있었다. 한편, 비소는 급성전골수성 백혈병의 치료제로 사용되면서 암 치료제로써의 비소 작용 기전 연구도 활발하게 이루어지고 있다. 하지만 비소의 암세포 사멸 효과는 혈액세포 유래 암에서 한정적이며 고형종양에서는 효과를 보이는 비소의 농도가 높아 사용이 제한적이다. 본 연구에서는 비소의 간암세포에서의 세포사멸 유발 기전에 대한 연구의 하나로 비소에 의한 Akt 단백질의 발현 감소와 GSK3β 신호체계와의 관련성을 확인하였다. 비소는 간암, 결장암, 전립선암, 자궁경부암 유래 세포에서 세포 사멸과 Akt의 감소를 유발하였다. 비소의 의한 세포사멸은 항산화제에 의해 경감되며 Akt의 감소는 GSK3β의 활성화에 의한 것임을 siRNA를 이용하여 확인하였다. 이상의 결과는 비소가 여러 신호전달체계를 통해 단백질 발현에 영향을 끼치며, 발현에 변화를 보인 단백질들이 비소에 의해 유발되는 질병 발생 및 치료 기전을 이해하는데 중요한 자료로 사용 될 수 있음을 시사한다.

주요어: 비소, 독성, HepG2 세포, 원숭이 간조직, 삼산화비소, 항암제
학번: 2008-21731